This is the Post-print Version
Hasnat, A., Islam, M. M., & Amin, A. F. M. S. (2015). Enhancing the Debonding Strain Limit for CFRP-Strengthened RC Beams Using U-Clamps: Identification of Design Parameters. Journal of Composites for Construction. http://dx.doi.org/10.1061/(ASCE)CC.1943-5614.0000599

Accepted for publication in the Journal of Composites for Construction, ASCE

Enhancing the Debonding Strain Limit for CFRP-Strengthened RC Beams Using U-Clamps: Identification of Design Parameters

A. Hasnat[1], M.M. Islam[2], A.F.M.S. Amin[3]
Department of Civil Engineering
Bangladesh University of Engineering and Technology, Dhaka 1000, Bangladesh

ABSTRACT

In simply supported reinforced concrete (RC) beams strengthened by carbon-fiber-reinforced polymer (CFRP) plates, plate debonding is initiated at the beam ends, where the principal compression, predominantly composed of a vertical component, detaches the plate externally bonded to the unconfined cover concrete. A CFRP wrap acting as a U-clamp can provide confinement to enhance the moment capacity by resisting premature cover debonding. The wrap design parameters in terms of clamping location, width and stiffness were identified from a set of fundamental experiments. The ultimate moment capacities of 22 tested specimens with different end anchorage conditions were compared against control specimens. The debonding strain, and consequently the ultimate moment capacity, gradually increased with increasing U-clamp width and stiffness. The failure patterns confirmed the effect of U-clamps in inducing a partial confinement effect on the sides and bottom of a beam end. The resulting changes in the compressive principal stress distribution in the compression arch were considered in formulating relationships for debonding strain prediction. The proposed relationship successfully predicted values regarding strengthened stone and brick aggregate concrete beams. The relationships for both unclamped and U-clamped anchorages better reproduced the experimental moment capacity enhancements than did the known equations. To assess the derived relations' wider applicability, the estimates obtained using the proposed relations were compared against published results for 42 test beams.

Author keywords: Brick aggregate concrete, Stone aggregate concrete, Confinement, Compression arch zone, Debonding strain prediction.

INTRODUCTION

The application of externally bonded carbon-fiber-reinforced polymer (CFRP) pultruded plates has emerged as a useful technique (see Roberts and Haji-Kazemi 1989 and Hussain et al. 1995 for an introduction to externally bonded steel plates, the forerunner of CFRP plates) for

[1] Graduate student
[2] Graduate student
[3]Corresponding author: Prof. Dr. A.F.M. Saiful Amin, Department of Civil Engineering, Bangladesh University of Engineering and Technology, Dhaka 1000, Bangladesh. Email: samin@ce.buet.ac.bd Fax: +880-2-9665639 Telephone: +880-2-9671155

enhancing the flexural capacity of reinforced concrete (RC) beams. In such applications, the plates, which are externally bonded to the 'unconfined cover concrete' at the tension face, often debond prematurely. In a simply supported beam, such a debonding phenomenon initiates at the beam ends near the face of the support, where both high normal stress and interfacial shear stress arise (Chajes et al. 1994, Arduini et al. 1997, Malek et al. 1998, Triantafillou 1998, Saadatmanesh and Malek 1998, Fanning and Kelly 2001, El-Mihilmy and Tedesco 2001, Smith and Teng 2002a,b, Lu et al. 2005, Esfahani et al. 2007, Yao and Teng 2007, Teng and Yao 2007, So and Harmon 2008).

Two methods of debonding prevention are commonly pursued at present (ACI 440.2R 2008). Following the first approach, Maruyama and Ueda (2001), Toutanji et al. (2006), ACI 440.2R (2008), Li et al. (2013) have proposed debonding models based on an extensive database of test results from lap shear tests and beam tests, for example, those of Chajes et al. (1994), Lu et al. (2005), and Li et al. (2013). These models attempt to limit the debonding strain, ε_{db}, with the intent of avoiding the phenomenon. Limiting debonding strain using such limits largely reduces the allowable flexural capacity enhancement, the target design parameter in a strengthening scheme. Following the second approach, Teng et al. (2003), Buyukozturk et al. (2004), Yalim et al. (2008), Al-Tamimi et al. (2011), Li et al. (2013) and Dong et al. (2013) have observed a distinct improvement in the flexural capacity of simply supported, strengthened beams that are clamped with U-clamps at the bottoms and sides of the beam ends. Spadea et al. (2001) have clamped externally bonded steel plates using CFRP wraps. In this latter approach, although the effects of the concrete surface preparation, concrete strength, clamping locations and clamping span have been extensively studied in detailed experiments, no agreement has been reached regarding a unified design approach established after considering the general stress situations in a beam rather than addressing only bond-slip behaviors (Lu et al. 2005, Li et al. 2013). Appropriate design parameters for such U-clamps in terms of their location, width, and thickness, which are necessary for the derivation of U-clamp design equations based on geometric properties, have not yet been identified. The lack of consensus in interpreting the related phenomena largely prevented any unified design approach from being proposed in *fib Bulletin 14* Approach 1 (2001) or ACI 440.2R (2008). Instead, a need for further research in this area was indicated.

In a simply supported RC beam, flexural capacity is generated by tied arch action, which only becomes effective when longitudinal tension reinforcement is appropriately anchored within the compression arch (using hooks/end plates/deformed bars providing adequate development length) at the end supports. Nevertheless, the placing of stirrups as internal shear reinforcement at beam ends, more often with a closer spacing, not only acts as shear reinforcement but also provides additional confinement to the longitudinal steel (Soroushian et al. 1991). In contrast, a plate externally bonded at the tension face with cover concrete has neither any mechanical anchorage nor any confinement to resist the principal compression unless U-clamps are appropriately attached to prevent debonding. In this context, the initiation of debonding at the support is regarded in this paper as analogous to the site at which diagonal tension cracks originate in an RC beam with no internal shear reinforcement, as reported in Figure 5 of Bower and Viest (1961), Figure 4 of Kani (1964) for stone aggregate concrete beams and Figure 2(c) of Akhtaruzzaman and Hasnat (1986) for brick aggregate concrete beams. Swamy et al. (1999) have experimentally demonstrated that externally bonded U-shaped CFRP/steel plate end

This is the Post-print Version
Hasnat, A., Islam, M. M., & Amin, A. F. M. S. (2015). Enhancing the Debonding Strain Limit for CFRP-Strengthened RC Beams Using U-Clamps: Identification of Design Parameters. Journal of Composites for Construction. http://dx.doi.org/10.1061/(ASCE)CC.1943-5614.0000599

anchorages and separate laterally bolted steel confinement plates at mid-span above the neutral axis covering the entire compression arch zone of a simply supported RC beam bonded to external plates at the tension face can fully prevent the brittle shear failure of the beam without any internal shear reinforcement. Ductile flexural failure can thereby be achieved. Bencardino et al. (2002) reconfirmed this assertion and emphasized the need to enhance the compression zone capacity by means of appropriate confinement arrangements in the form of U-clamps and lateral confinements to enhance the limiting debonding strain, ε_{db}. Nevertheless, in such an approach, the compression arch of the beam and its transformation upon the introduction of a CFRP plate at the tension face and U-clamps as end anchorages must be considered from a general perspective. Furthermore, a certain lack of clarity exists in the requirements for limiting the debonding strain in strengthened beams because of the variations in the quality of the aggregates (So and Harman 2008) used to make the concrete itself. Over the past six decades, the severe scarcity of natural stones suitable for use as coarse aggregates in concrete that is encountered in Bangladesh and some parts of India, where the land is formed of recent sedimentary deposits, has forced crushed burnt clay bricks to be used as an alternative to stone aggregates (Akhtaruzzaman and Hasnat 1983, Mansur et al. 1999, Khalaf and DeVenny 2005, Khalaf 2006, Debieb and Kenai 2008). Islam et al. (2011 and 2015) and Choudhury (2012) have reported that the dilation effect in confined brick aggregate concrete under compression is significantly larger than that in stone aggregate concrete. This finding demands a careful review of unclamped and U-clamped CFRP-strengthened RC beams formed from this type of concrete to allow for an appropriate evaluation of the limits on the debonding strain, ε_{db}.

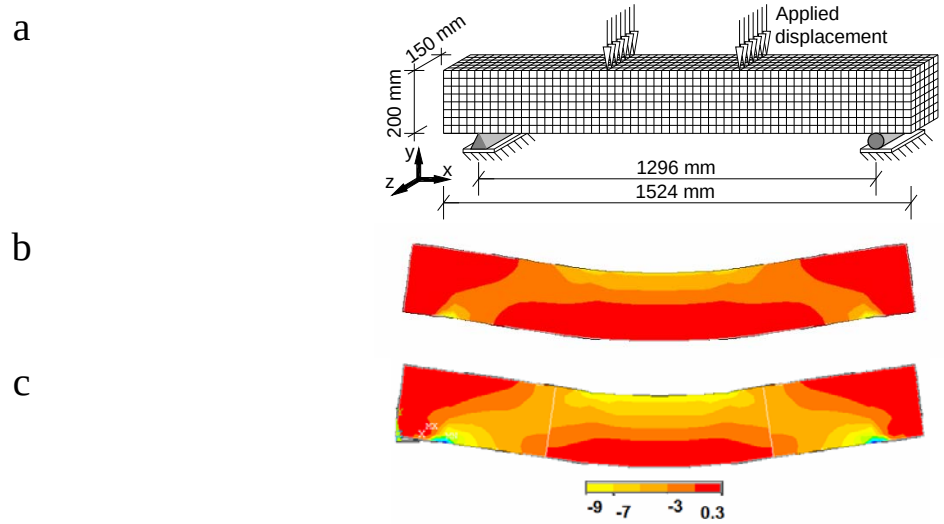

Fig. 1. Variations in the stress distribution caused by end anchorages, as obtained via the finite element (FE) analysis of a simply supported beam. (a) FE model. The sides of each square in the depicted grid were divided in two to generate the mesh. (b) Principal compression stress contours in a plain concrete beam with $f_c^{'}$ = 48 MPa. (c) Principal stress (compression) contours in a beam whose two ends (25% of the beam span) possess a higher concrete strength ($f_c^{'}$ = 240 MPa). The middle section consists of 48 MPa concrete.

This is the Post-print Version
Hasnat, A., Islam, M. M., & Amin, A. F. M. S. (2015). Enhancing the Debonding Strain Limit for CFRP-Strengthened RC Beams Using U-Clamps: Identification of Design Parameters. Journal of Composites for Construction. http://dx.doi.org/10.1061/(ASCE)CC.1943-5614.0000599

COMPRESSION ARCHES, DEBONDING PHENOMENA AND CONFINEMENT

The basic concept of the compression arch in a simply supported beam under four-point loading and the transformation of this arch due to additional confinement in the form of U-clamp end anchorages are illustrated in Figure 1. To do this, a numerical analysis was performed using ANSYS Version 11, a general-purpose finite element software package. A homogeneous concrete beam was modeled using the SOLID65 element in Figure 1(a). The sides of each square in the depicted grid were divided in two to generate the mesh. The Willam-Warnke yield criterion was used together with the Newton-Raphson approach to obtain the simplest nonlinear solution to the problem. The application of a displacement control algorithm up to the maximum possible displacement level (25 mm) yielded a converged solution. Figure 1(b) shows that the principal compression (plain concrete beam with $f_c^{'}$ = 48 MPa) is predominantly vertical at the support, where debonding is known to initiate. The vertical and horizontal components gradually decrease and increase, respectively, away from the support toward the mid-span. To incorporate the possible theoretical confinement effect of CFRP U-clamps acting as end anchorages, both ends of the beam were assigned higher compressive strengths ($f_c^{'}$ = 240 MPa), as shown in Figure 1(c). The middle section consists of 48 MPa concrete. A comparison of the principal stress contours presented in Figures 1(b) and 1(c) reveals a remarkable increase in the extent of the arch-shaped compression zone (compression arch) in the regions near the supports.

The general stress situation is further illustrated schematically in Figure 2 for RC beams. Three stress situations are compared. An unstrengthened (control) beam and CFRP-strengthened beams both with and without end anchorages are considered, yielding seven possible failure patterns (I–VII) and their corresponding locations. Figure 2(a) shows the fundamental tied-arch action in a simply supported RC beam with the ends of the tension reinforcement embedded within the compression arch. The shift in the compression zone caused by U-clamps at beam ends is illustrated in Figure 2(b). U-clamps are provided by unidirectional CFRP wraps aligned along the beam perimeter. The resultant stresses governing the section capacities in the two cases are compared in Figure 2(c). Failure pattern II [Figure 2(b)] represents typical cover debonding, as observed in unclamped beams as a result of principal compression that has the predominant vertical component at the ends to initiate debonding [Figure 1(b)]. After the introduction of the U-clamp, a progressive failure should occur with gradually increasing load. The vertical component of the principal compression resisted by the U-clamp generates failure pattern IV [Figure 2(c)]. Failure patterns III, IV and V are associated with the bursting off of the cover concrete around the beam perimeter, where it is confined only by CFRP-wrap U-clamps, as reported by Swamy et al. (1999), Al-Tamimi et al. (2011) and Hasnat (2014). These failure patterns are analogous to those observed in the confinement failure of CFRP-jacketed compression members (see Islam et al. 2015 and the references cited therein), and they vividly illustrate the effect of U-clamps in inducing a partial confinement effect (Pessiki et al. 2001; Braga et al. 2006) and thus an increase in the “apparent” compressive strength (Mirmiran and Shahawy 1997a,b, Mirmiran et al. 1998, Wu and Wei 2010; Moran and Pantelides 2005, ACI 440.2R 2008, Girgin 2009, Toutanji et al. 2010) observed near the U-clamp application zone. In the present work, the authors were motivated by this mechanics-based physical interpretation to arrive at more fundamental governing relations that incorporate the geometric dimensions and material parameters of CFRP wraps into the detailed design of U-clamps.

This is the Post-print Version
Hasnat, A., Islam, M. M., & Amin, A. F. M. S. (2015). Enhancing the Debonding Strain Limit for CFRP-Strengthened RC Beams Using U-Clamps: Identification of Design Parameters. Journal of Composites for Construction. http://dx.doi.org/10.1061/(ASCE)CC.1943-5614.0000599

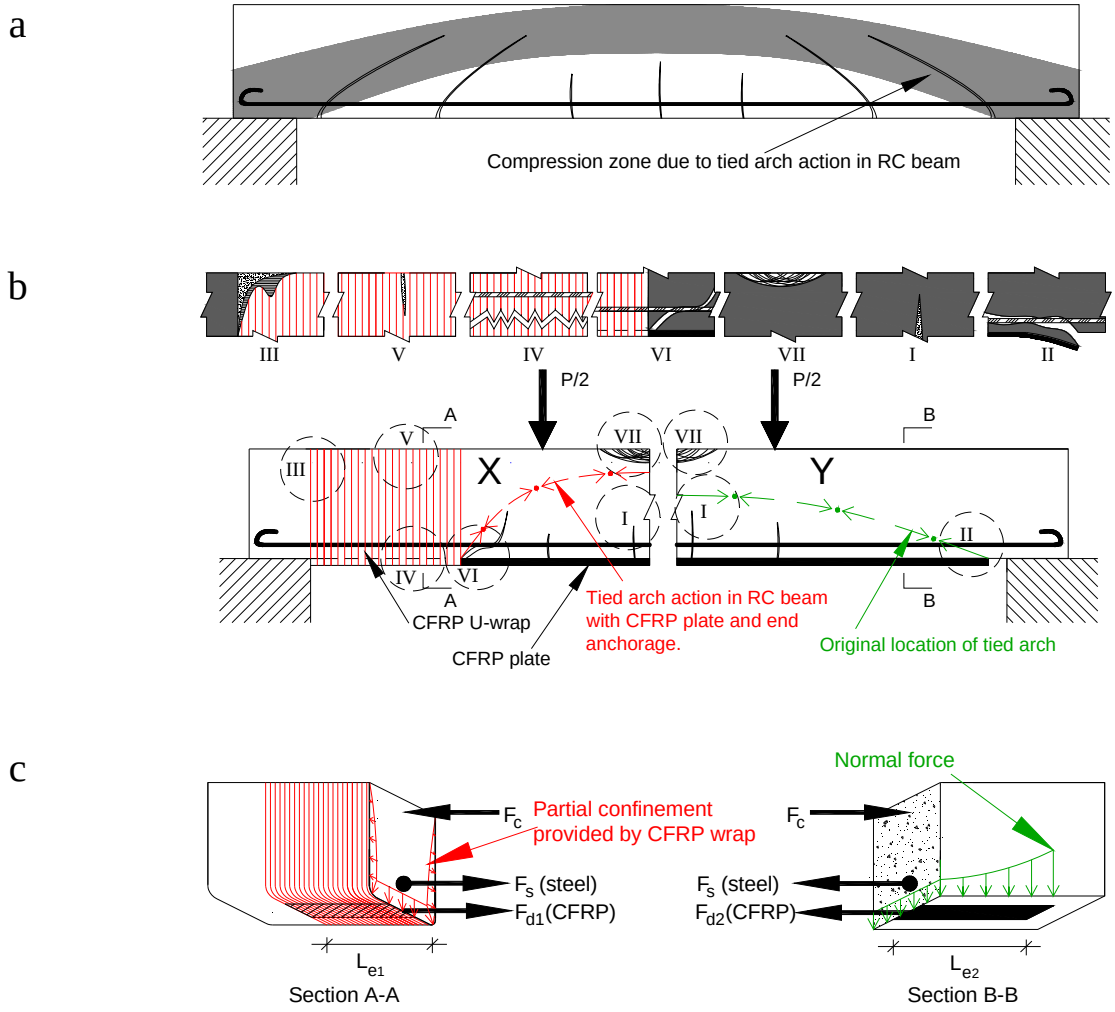

Fig. 2. Schematic representation of the stress distributions in RC beams: (a) the compression zone in an unstrengthened beam and (b) the failure patterns (I-VII) at different locations on CFRP-plate-strengthened RC beams with U-clamp end anchorage (X) and without end anchorages (Y). (c) The probable reorientation in stress distribution induced by the introduction of CFRP wraps acting as U-clamps.

OBJECTIVES AND METHODOLOGY

The purpose of the current work was to observe the fundamental phenomena (Figures 1–2) occurring in a set of experiments conducted on simply supported RC beams made of brick and stone aggregates. Unstrengthened (control) beams, unclamped CFRP-strengthened beams and U-clamped beams strengthened with pultruded CFRP plates were tested under four-point loading. The U-clamps consisted of unidirectional CFRP wraps around the sides and bottoms of the beams, and the wraps were varied in location, width and stiffness. The results obtained from the tests were synthesized to observe the effects of the coarse aggregates as well as the progressive change in moment capacity induced by the gradual incorporation of U-clamp end anchorages. The forms of the relations among the principal compressive stress, the normalized wrap width and the confined compressive strength due to CFRP U-clamping were established. The coefficients in these relations were explicitly estimated from first-hand test data. The

performances of the equations thus derived for estimating the debonding strains, ε_{db}, for unclamped and U-clamped beams were compared with the known equations in terms of their ability to reproduce the moment capacities measured in the tests. Finally, the moment capacities obtained using the derived equations for different test beams under different test conditions corresponding to data available in the published literature were critically assessed and interpreted in an independent performance evaluation.

EXPERIMENTAL STUDY

This section describes an experimental study motivated by the foregoing discussions for the validation of the predicted phenomena and the acquisition of first-hand data from which to derive design equations to determine the limiting debonding strain, ε_{db}, in unclamped and U-clamped simply supported beams.

Experimental plan

This sub-section describes a test scheme that allowed for the observation of the effect of variations in the governing parameters (Figure 3) on the ultimate moment capacities of the test beams. The first column of the figure provides elevation and cross-sectional views of the test beams together with the anchorage and strengthening schemes. Side and bottom views of the anchorage schemes are illustrated in the two columns to the right, along with the details of the CFRP wrap mounting techniques in a sectional view. Symbols for the control and strengthened beams manufactured using brick aggregate concrete (B) and stone aggregate concrete (S) are noted in the two rightmost columns. The notations 1W and 2W indicate single and double layers of wrap, respectively. Reinforcement details are shown in Figure 4. The notations C and T represent beams that were weak in the compression zone and strong in the compression zone, respectively (Figures 3 and 4).

In addition to unstrengthened (control) beams (Figure 3a), three general types of anchorage systems, namely, Anchorage Type 1 (AT1), Anchorage Type 2 (AT2) and Anchorage Type 3 (AT3a, 3b, 3c, 3d), for brick aggregate and stone aggregate concrete beams were tested under four-point loading (Figure 3). The installation of externally bonded plates on the tension side with different types of end anchorages was intended to enhance the flexural capacity to different extents in the different test specimens. To avoid debonding, mechanical anchorages (analogous to hooks or end plates in RC beams) are often deployed in practice (Kalfat et al. 2013). The AT2 beams (mechanical clamping at the reaction point) were tested to acquire data corresponding to a scenario between AT1 (no clamping) and AT3 (distributed clamping with CFRP wraps) to compare the efficacy of such a mechanical anchorage system with the confinement effect achievable using U-clamps, as hypothesized in Figures 1–2. In AT3a–d, the numbers, widths, locations and stiffnesses (proportional to the number of wrap layers) of the U-clamps were varied. To facilitate confinement, the beam corners were rounded at a 25 mm radius (Figure 3) following the customary procedure for confining RC columns (ACI 440.2R 2008). All U-clamps were extended up to the top edge corners of the beams, the maximum practical limit. This is well above the upper boundary of the principal compression arch (Figure 1), thus offering a variable amount of lap length along the beam axis.

This is the Post-print Version
Hasnat, A., Islam, M. M., & Amin, A. F. M. S. (2015). Enhancing the Debonding Strain Limit for CFRP-Strengthened RC Beams Using U-Clamps: Identification of Design Parameters. Journal of Composites for Construction. http://dx.doi.org/10.1061/(ASCE)CC.1943-5614.0000599

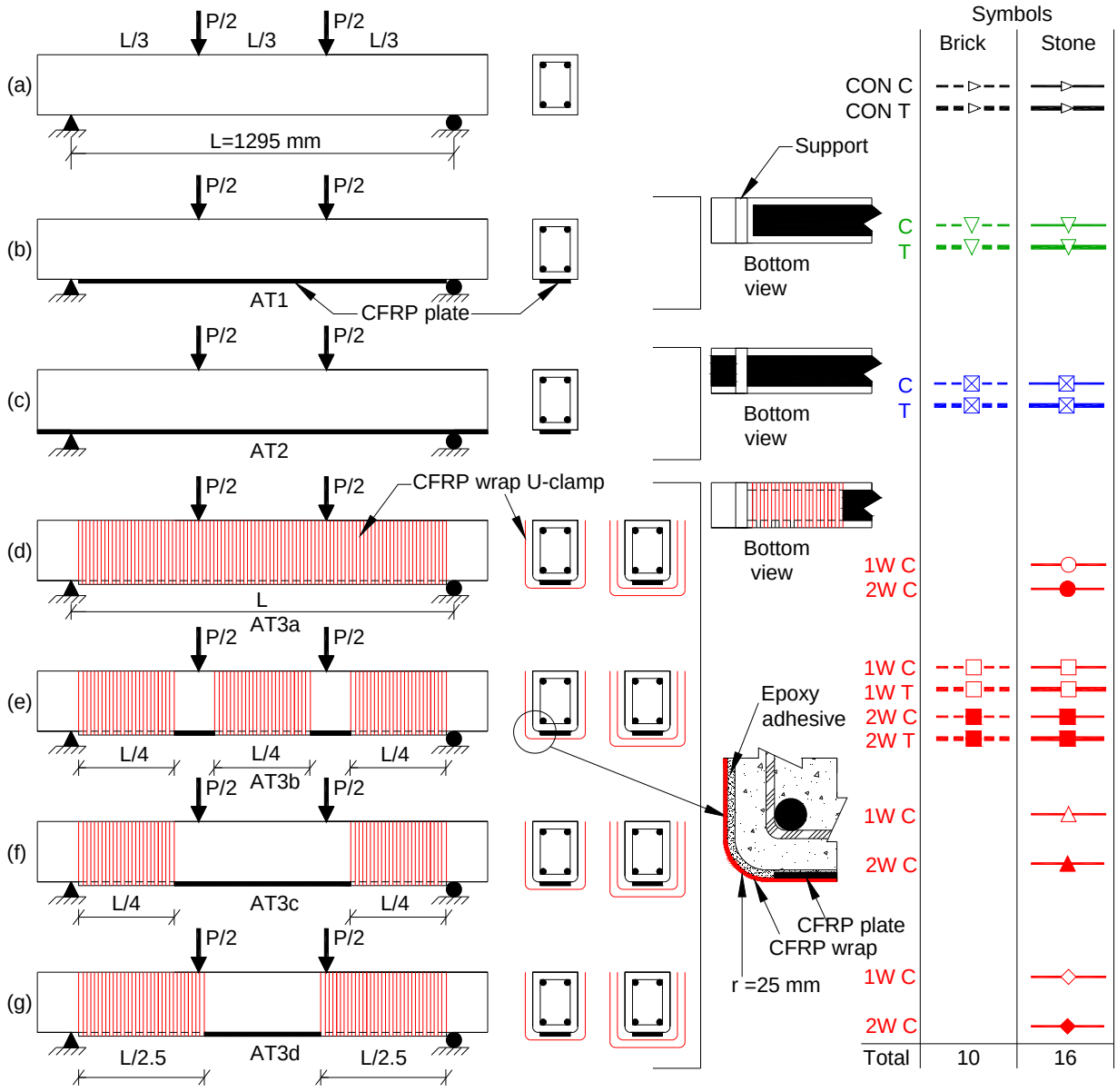

Fig. 3. Details of the test specimens, supports and loading conditions: (a) control specimen; (b) strengthened unclamped beams, AT1; (c) strengthened beams with mechanical anchorage, AT2; (d) strengthened U-clamped beams, AT3a; (e) strengthened U-clamped beams, AT3b; (f) strengthened U-clamped beams, AT3c; and (g) strengthened U-clamped beams, AT3d.

The application of a U-clamp along the full length of the test beam, as shown in Figure 3(d) for AT3a, is comparable to the scheme used for Beams NS3, NS4 and NS5 by Swamy et al. (1999). The U-clamps on the test beams shown in Figure 3(e) and 3(f) for AT3b and AT3c do not fully extend to the loading point, a test condition comparable to those reported by Al-Tamimi et al. (2011). The U-clamps on the test beams shown in Figure 3(g) for AT3d extend beyond the loading point, to the farthest extremity of the compression arch along the shear span. Thus, Figure 3(g) is closely comparable to Beam NS1 of Swamy et al. (1999). To assess the effect of

This is the Post-print Version
Hasnat, A., Islam, M. M., & Amin, A. F. M. S. (2015). Enhancing the Debonding Strain Limit for CFRP-Strengthened RC Beams Using U-Clamps: Identification of Design Parameters. Journal of Composites for Construction. http://dx.doi.org/10.1061/(ASCE)CC.1943-5614.0000599

the CFRP wrap thickness, the test beams depicted in Figures 3(d-g) were prepared with both single and double layers of wrap.

Figure 4 provides the reinforcement details. All beams were over-reinforced for shear capacity. The compression sides of several of the beams were made stronger with additional reinforcements, whereas the remainders of the beams were given the same amount of reinforcement on both the compression and tension sides. The purpose of preparing strong compression sides was to investigate whether any ductile flexural failure could be achieved by forming a strong compression arch in any of these strengthened test beams. The symbols defined in Figure 3 are used in all figures to present the test data throughout this paper.

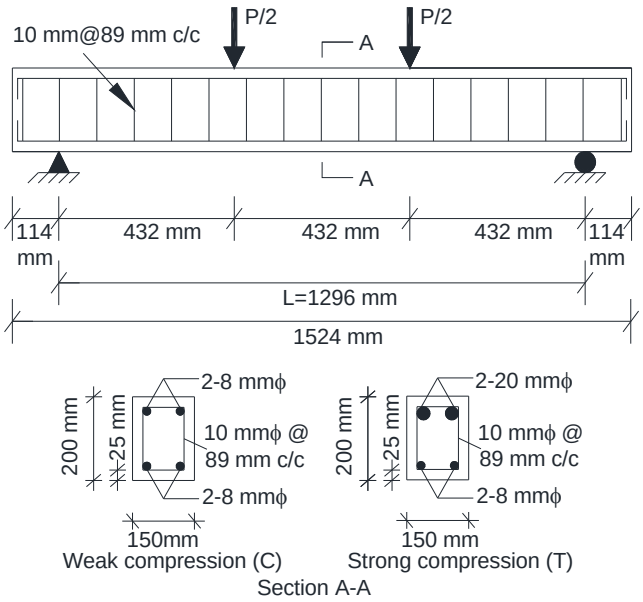

Fig. 4. Typical beam specimens and their steel reinforcement schemes. The reinforcements for weak-compression-zone (C) and strong-compression-zone (T) specimens are shown in Section A-A. This figure should be read in conjunction with Figure 3.

Materials

Crushed stone aggregate and crushed brick aggregate were used as the coarse aggregates for casting the concrete. Riverbed sand (fineness modulus of 2.6) was used as the fine aggregate. Ordinary Portland cement was used as the binding material ASTM C150/C150M (ASTM 2012). The basic engineering properties of the coarse aggregates are given in Table 1. The Los Angeles Abrasion (LAA) values of brick are typically higher than those of stone aggregates because of the higher porosity and lower unit weight of brick. Steel reinforcements with a yield strength of 414 MPa (Figure 5) were used. Table 2 shows the strengths of the concretes made with brick (B) and stone (S) aggregates. Compressive strengths ($f_c^{'}$) were determined per ASTM C39/C39M (ASTM 2014). Split tension strengths (f_t) were determined using ASTM C496/C496M (ASTM 2011). Pull-off strengths (f_{tp}) were determined using ASTM D4541 (ASTM 2009). The concrete mix ratio (v/v) was maintained at 1:1.25:2.50, and the water-cement ratio was 0.45.

This is the Post-print Version
Hasnat, A., Islam, M. M., & Amin, A. F. M. S. (2015). Enhancing the Debonding Strain Limit for CFRP-Strengthened RC Beams Using U-Clamps: Identification of Design Parameters. Journal of Composites for Construction. http://dx.doi.org/10.1061/(ASCE)CC.1943-5614.0000599

The engineering properties of the pultruded CFRP plates, which were of uniform thickness, were tested per ASTM D3039/D3039M (ASTM 2014). The properties useful for design are summarized in Table 3 for the pultruded CFRP plates and dry carbon fibers. Dog-bone specimens were prepared as per ASTM D638 (ASTM 2010) for strength tests of adhesive and primer used to install CFRP plates. Figure 5 presents the stress-strain responses of the concretes, reinforcing steel, CFRP plate, adhesive and primer. The values of the modulus of elasticity, E, for the adhesive and primer are the lowest, whereas that of the CFRP plates is the highest, with those of the two types of concretes in between. Brick aggregate concrete is characteristically softer than stone aggregate concrete (Akhtaruzzaman and Hasnat 1983, Mansur et al. 1999, Islam et al. 2015).

Table 1. Properties of coarse aggregates.

Type of coarse aggregate	LAA* value (%)	Absorption capacity (%)	Bulk specific gravity (OD)	Bulk specific gravity (SSD)	Unit wt. kg/m^3
Stone	29.5	0.8	2.6	2.6	1568
Brick	38.0	14.4	1.9	2.1	1110

*Los Angeles Abrasion value

Table 2. Properties of concrete.

Concretes (ID)	f_c' (MPa)	f_t (MPa)	f_{tp} (MPa)
Stone aggregate concrete (S)	48.3	3.5	3.3
Brick aggregate concrete (B)	47.5	3.8	3.8

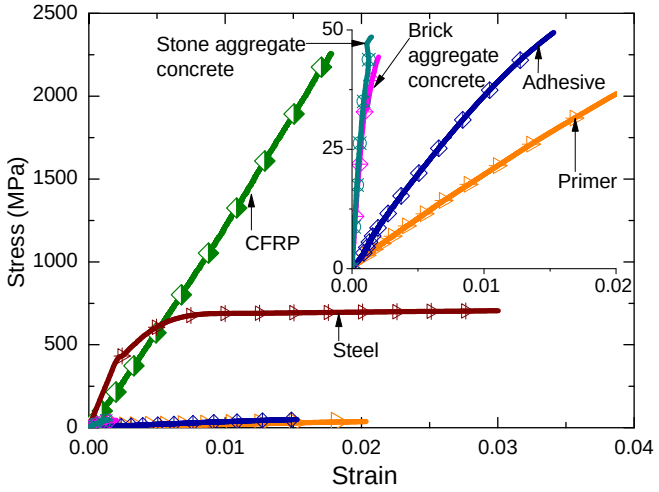

Fig. 5. Stress-strain responses of primer, adhesive, CFRP plate, steel, brick aggregate concrete and stone aggregate concrete. Further illustration of the responses of the concretes, adhesive and primer is provided in the inset figure.

Preparation of RC beam specimens

The concrete mixes were prepared in different batches in a gravity mixer. After the green concrete was placed in the steel formwork, compaction was achieved using a vibrator. To assess

This is the Post-print Version
Hasnat, A., Islam, M. M., & Amin, A. F. M. S. (2015). Enhancing the Debonding Strain Limit for CFRP-Strengthened RC Beams Using U-Clamps: Identification of Design Parameters. Journal of Composites for Construction. http://dx.doi.org/10.1061/(ASCE)CC.1943-5614.0000599

the strength properties, cylinder specimens were also prepared from each batch. All beams and cylinders were removed from their steel molds 24 h after casting and cured in lime water for 28 days. The design compressive strength was 48 MPa. The brick aggregate concrete attained a slightly lower compressive strength but a higher tensile strength than did the stone aggregate concrete (Table 2).

Table 3. Material properties of CFRP, adhesive, and primer

Material	f_u (MPa)	E (GPa)	ε^*_{fu} (%)	Thickness, t (mm)	Width (mm)
CFRP plate (pultruded)	2260	120	1.7	1.2	100
Dry carbon fiber#	4300	240	1.5	0.275	-
Adhesive	48.3	4.4	1.5	-	-
Primer	35	2.5	2.1	-	-

#Manufacturer's technical data sheet

Strengthening of RC beams

The CFRP plates (LaMaCo System Sdn Bhd, Malaysia) and wraps (Fosroc Chemicals Pvt. Ltd., India) were installed on the grinded surfaces (ACI 440.2R 2008) of the test beams in accordance with the respective manufacturer's technical data sheets to install plate and wrap systems. The individual components of the adhesive and primer were mixed following the manufacturer's technical data sheets. The pultruded CFRP plates were installed using a 2 mm thick epoxy adhesive layer. Pressure was applied to the CFRP plates using a roller to squeeze out any excess adhesive. Three days after the installation of the CFRP plates, the dry carbon fibers impregnated in the epoxy adhesive were wrapped around the beams to form U-clamps, in accordance with the details shown in Figure 3. The adhesion among the base concrete, CFRP plate and wrap was confirmed via pull-off tests. The results are summarized in Table 2, where in each case, concrete failure in the pull-off test confirmed sound adhesion. Figure 6 presents several specimens after CFRP installation. A few control specimens are also partially visible in the figure.

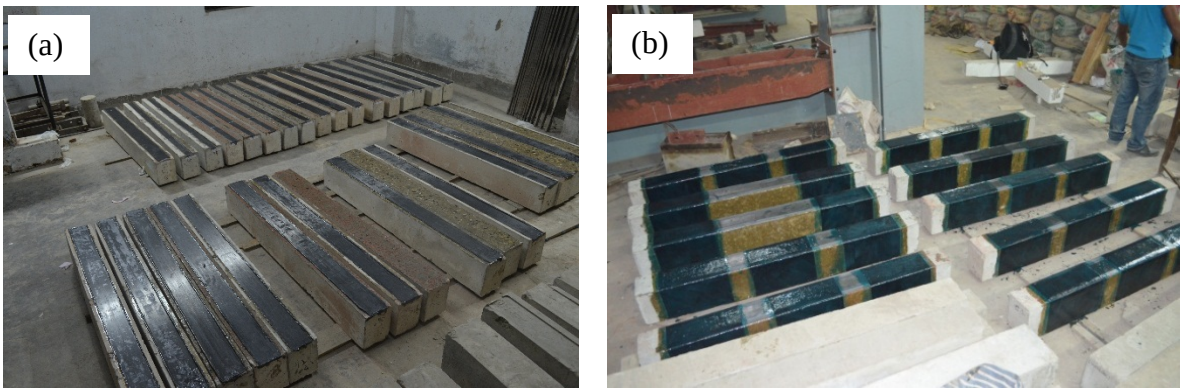

Fig. 6. Test specimens: (a) beams strengthened with laminated CFRP plates (AT1 and AT2) and (b) beams strengthened with laminated CFRP plates and U-clamp anchorages (AT3b–d).

Testing and data acquisition

All beams were tested using a computer-controlled universal testing machine (Tinius Olsen Testing Machine Company, Horsham, PA 19044, USA) by applying displacements at a rate of 1 mm/min. The specimens were tested under four-point loading (Figure 7). A rubber pad was placed at the support point of the beam to minimize the stress concentration. The axial load and

This is the Post-print Version
Hasnat, A., Islam, M. M., & Amin, A. F. M. S. (2015). Enhancing the Debonding Strain Limit for CFRP-Strengthened RC Beams Using U-Clamps: Identification of Design Parameters. Journal of Composites for Construction. http://dx.doi.org/10.1061/(ASCE)CC.1943-5614.0000599

vertical displacement data from the load cell were recorded by a computer. The strain history across the beam depth at zero shear zone (mid-zone) was recorded using a video extensometer system (Tinius Olsen Testing Machine Company, Horsham, PA 19044, USA). This system was also connected to the same computer for the acquisition of a unique load-displacement-strain measurement history. The failure patterns of the specimens were recorded using a high-definition video camera in each test.

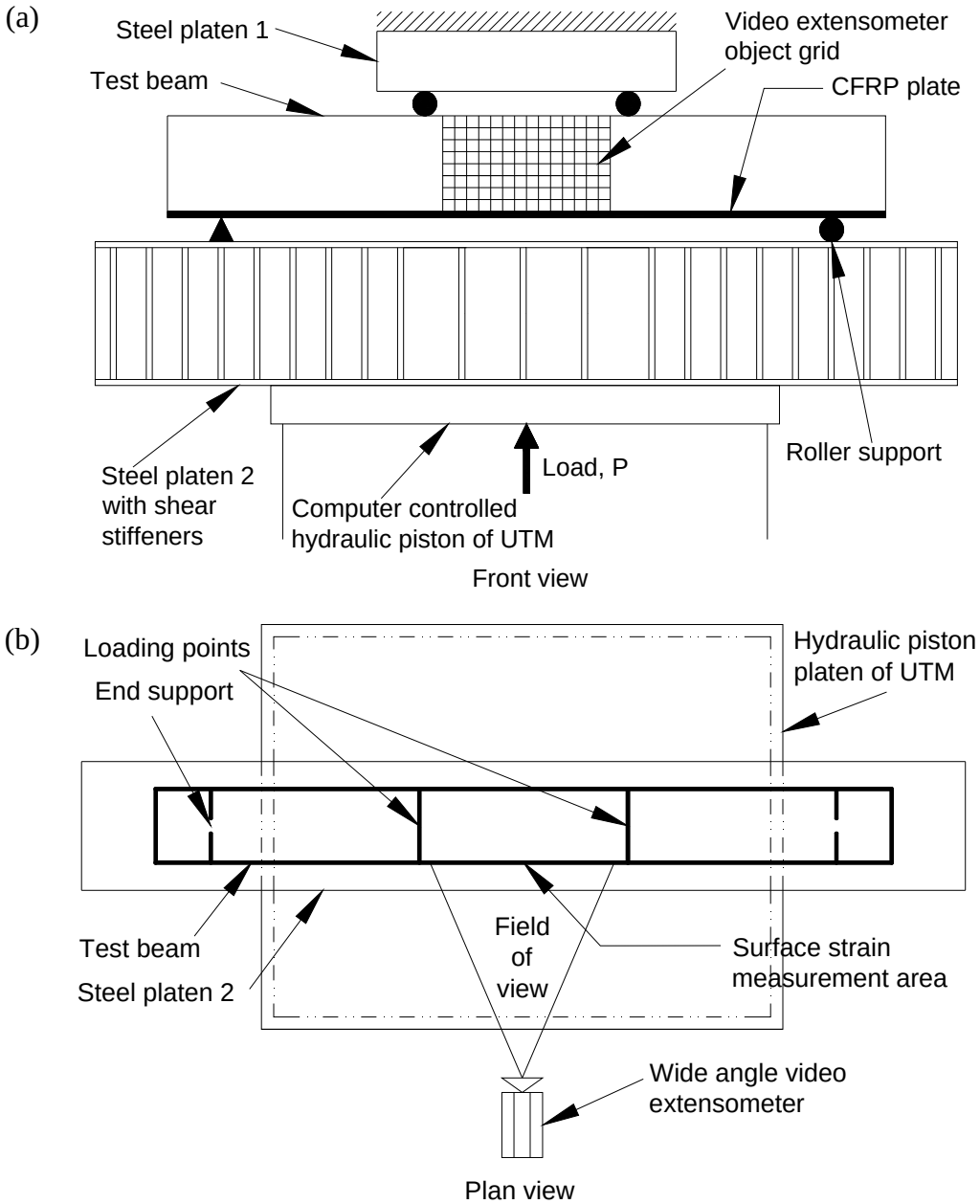

Fig. 7. Test setup for testing the beams: (a) plan view and (b) front view. A schematic illustration is provided, showing an AT2 specimen mounted on the test rig.

This is the Post-print Version
Hasnat, A., Islam, M. M., & Amin, A. F. M. S. (2015). Enhancing the Debonding Strain Limit for CFRP-Strengthened RC Beams Using U-Clamps: Identification of Design Parameters. Journal of Composites for Construction. http://dx.doi.org/10.1061/(ASCE)CC.1943-5614.0000599

RESULTS AND DISCUSSION

Test results

The cardinal photographs of the failure patterns are presented Figure 8. The load, deflection and stiffness data measured in the tests are tabulated in Table 4. The changes in the ultimate load, deflection, strain over the beam depth and stiffness are plotted and critically evaluated in Figures 9-10. Parity plots are provided for beams made using the two types of coarse aggregates and two different reinforcement schemes (Figure 11). The results from test beams of identical geometry and concrete strength but varied anchorage conditions are compared in Figure 12. The unstrengthened control RC beams, unclamped RC beams and clamped RC beams with variations in their clamping parameters were all tested using the same test protocol.

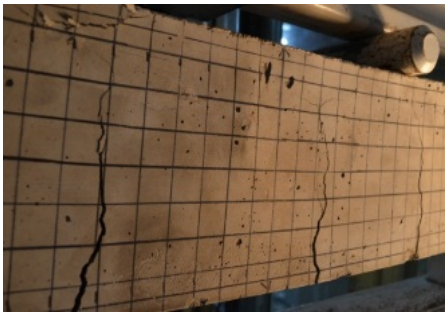

Failure Pattern I

Failure Pattern II & VII

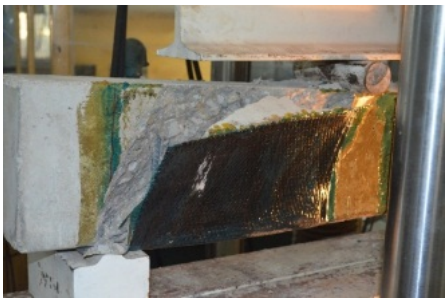

Failure Pattern III

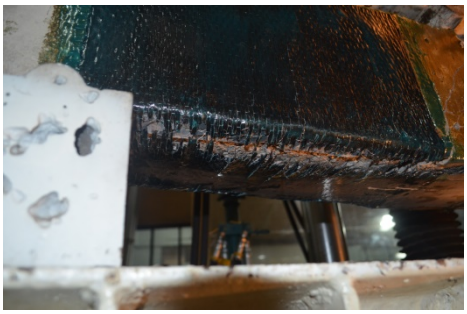

Failure Pattern IV

Failure Pattern V

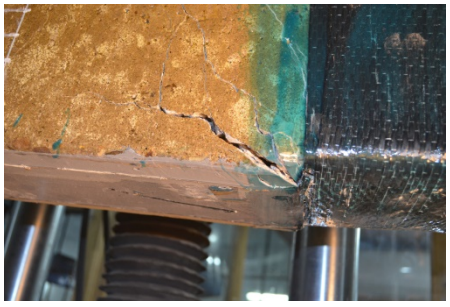

Failure Pattern VI

Fig. 8. Typical failure patterns (I–VII) in unstrengthened RC beams, strengthened unclamped RC beams and strengthened RC beams with U-clamps. The figure should be read in conjunction with Figure 2.

Failure patterns and debonding phenomena

Photographs of the typical failure patterns (summarized in Figure 2) observed at different locations during the tests are provided in Figure 8 and Table 4. No visible shear cracking was observed in any of the specimens [except S(AT3d)2WC] because the specimens were designed to resist shear failure. The failures of the control (unstrengthened) specimens were initiated by the yielding of the steel (failure pattern I), whereas the failures of all of the strengthened unclamped beams (AT1) were dominated by cover debonding (failure pattern II). Typically, such debonding in the CFRP plate-strengthened beams occurred in zones near the supports, where the compression arch met the plate that was externally bonded to the unconfined cover concrete (see also Arduini et al. 1997, Fanning and Kelly 2001, Smith and Teng 2002a, Alagusundaramoorthy et al. 2003, So and Harmon 2008). Moreover, all longitudinal steel reinforcements remained confined within the internal shear reinforcement, whereas the externally bonded plates remained unconfined in AT1 specimens.

Table 4. Ultimate loads sustained by different specimens and their failure modes.

Specimen ID	Anchorage type[#]	P (kN)	Deflection at P (mm)	Stiffness (kN/mm)	Failure pattern[*]
S(CON)C	Control	34.2	4.8	9.5	I
S(CON)T	Control	36.4	4.8	12.0	I
B(CON)C	Control	37.8	5.0	11.1	I
B(CON)T	Control	35.5	5.3	7.3	I
S(AT1)C	AT1	100.0	6.2	14.3	II
S(AT1)T	AT1	100.4	7.0	12.0	II
B(AT1)C	AT1	101.6	7.1	14.3	II
B(AT1)T	AT1	100.4	7.2	11.5	II
S(AT2)C	AT2	112.9	9.8	11.0	II
S(AT2)T	AT2	133.1	8.5	16.0	II
B(AT2)C	AT2	108.5	7.7	8.0	II
B(AT2)T	AT2	127.2	10.5	20.0	II
S(AT3a)1WC	AT3a	140.6	9.3	19.5	III
S(AT3a)2WC	AT3a	137.1	15.6	19.4	III
B(AT3b)1WT	AT3b	133.1	10.0	20.7	IV
B(AT3b)1WC	AT3b	142.9	9.2	24.3	IV
S(AT3b)1WC	AT3b	151.2	10.5	18.0	V
B(AT3b)2WT	AT3b	160.0	14.0	18.5	III
S(AT3b)1WT	AT3b	160.1	11.0	22.5	V
B(AT3b)2WC	AT3b	160.4	10.0	14.0	III
S(AT3b)2WT	AT3b	150.8	11.0	22.4	V
S(AT3b)2WC	AT3b	165.3	10.7	22.4	V
S(AT3c)1WC	AT3c	130.4	8.1	25.0	IV
S(AT3c)2WC	AT3c	162.9	10.7	20.1	IV
S(AT3d)1WC	AT3d	167.7	11.2	22.5	IV
S(AT3d)2WC	AT3d	198.9	12.4	18.6	VI

* Photographs of Failure Patterns are presented in Figure 1. #Anchorage types are illustrated in Figure 4. Notations: S: stone aggregate concrete; B: brick aggregate concrete; CON: control specimen; C: specimens weak in compression; T: specimens strong in compression; 1W: single layer wrap; 2W: double layer wrap. Notations are further detailed in Figure 4.

Hasnat, A., Islam, M. M., & Amin, A. F. M. S. (2015). Enhancing the Debonding Strain Limit for CFRP-Strengthened RC Beams Using U-Clamps: Identification of Design Parameters. Journal of Composites for Construction. http://dx.doi.org/10.1061/(ASCE)CC.1943-5614.0000599

The CFRP plates at the beam ends were mechanically anchored at the reaction points in the group of beams with the AT2 end anchorage type. However, the beams in this group also failed following failure pattern II. This observation clearly indicates that (i) the reaction force that acts as a mechanical anchorage is exactly same as the principal compression at the line of support and (ii) the reaction force acts as a mechanical anchorage only along a line, and the compression zone beyond that line remains unconfined.

The incorporation of U-clamps at different locations and stiffnesses in the AT3 specimens enhanced the capacity to different extents, resulting in diverse failure patterns (failure patterns III–VI). Failure patterns III–V (see also Table 4) illustrate the role of U-clamps in mobilizing partial confinement in the debonding zone where they are installed. With increasing U-clamp stiffness in the S(AT3d)2WC, shear cracks (failure pattern VI) were observed at the end of the U-clamp once the applied load exceeded the shear capacity of the test beam. Concrete failures in the compression zone were identified as failure pattern VII.

Verification of failure patterns and ultimate loads in comparison with the literature

The failure patterns reported in this paper for AT3 and their contrasts with those for AT1 and AT2 provide first-hand evidence suggesting approaches to addressing the issue from a more general perspective. First, for the AT3 beams, the photographs clearly show the bursting off of the concrete cover around the perimeter of a beam confined by CFRP-wrap U-clamps (failure patterns III, IV and V, Figure 8). These observations are in complete agreement with those independently reported by Swamy et al. (1999) in Figure 6 for NS1 specimen and Al-Tamimi et al. (2011) in Figure 3(g) for B0PWD specimen. In unclamped case (AT1), the cover concrete together with the plate separates only from the bottom of the beam (failure pattern II, Figure 8). Thus, the effectiveness of U-clamps in generating the desired clamping effect against debonding action is shown to be governed by the principal (compression) stress distribution, represented by the compression arch. Nevertheless, the test beams for the AT3a and AT3b cases were also installed with a U-clamp at the mid-span, with the fibers aligned perpendicular to the direction of principal compression above the neutral axis and to the direction of principal tension below the neutral axis. The resulting incompatibility in the stress/strain situation may provide an explanation for the lack of any significant capacity enhancement in these cases. In this context, the experiments of Swamy et al. (1999) for the test pieces labeled as Beams NS3, NS4 and NS5 can be revisited once again; in these experiments, steel plates attached to the sides of a beam using transverse bolts (across the beam width) only above the neutral axis, and hence confining only the compression arch, were found to be effective in providing sound lateral confinement for the arch. Furthermore, the test specimens with the AT3c scheme exhibited lower capacity enhancement than did the corresponding AT3d specimens, whose shear spans were better confined by the U-clamps. Furthermore, the concept of the location of U-clamp, shear span, confinement from U-clamp, direction of principal compression and orientation of wrap fiber as presented and discussed here can reasonably explain experiments of Al-Tamimi et al. (2011) in terms of ultimate load. Thus, the experiments of the authors are largely consistent with all the similar works known in literature in which, however, the interfacial shear stress and the normal compressive stress, the two major components of the principal stress, are considered individually.

This is the Post-print Version
Hasnat, A., Islam, M. M., & Amin, A. F. M. S. (2015). Enhancing the Debonding Strain Limit for CFRP-Strengthened RC Beams Using U-Clamps: Identification of Design Parameters. Journal of Composites for Construction. http://dx.doi.org/10.1061/(ASCE)CC.1943-5614.0000599

Load-displacement behavior

Figure 9 presents the load-displacement responses of beams made of brick aggregate concrete (Figure 9a–b) and stone aggregate concrete (Figure 9c–d) for different anchorage schemes (Figure 3) and steel reinforcement strategies (Figure 4). In general, the strengthened beams were not only stiffer but also sustained higher ultimate loads compared with the unstrengthened (control) beams. The strengthened beams also exhibited significantly larger displacements at the peak load, P, than did the control beams. The moment capacities predicted by ACI 440.2R (2008) for the beams strengthened using the AT1 scheme and by ACI 318 (2008) for the RC control beams are also plotted for comparison.

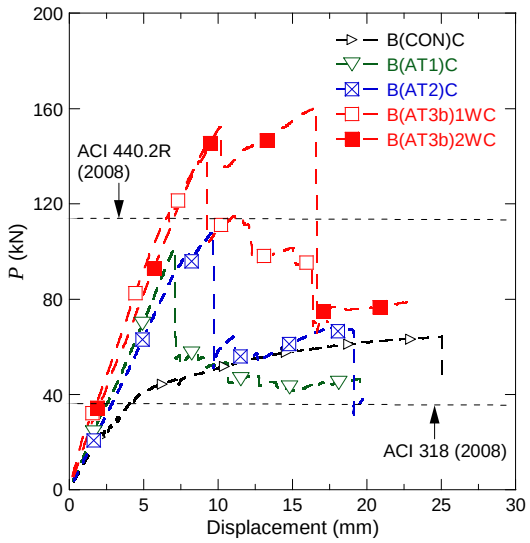

(a) Brick aggregate concrete (weak in compression)

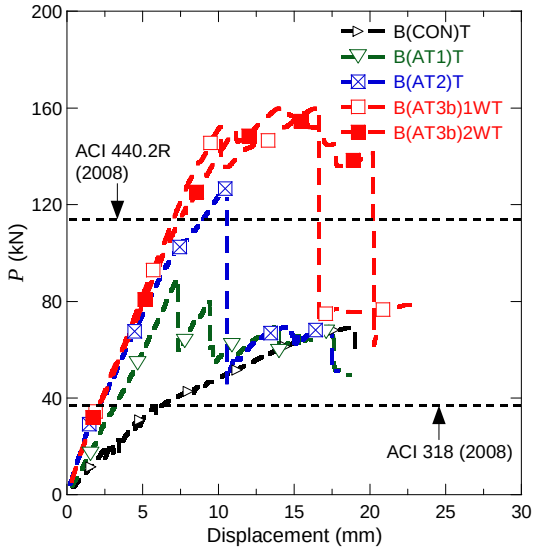

(b) Brick aggregate concrete (strong in compression)

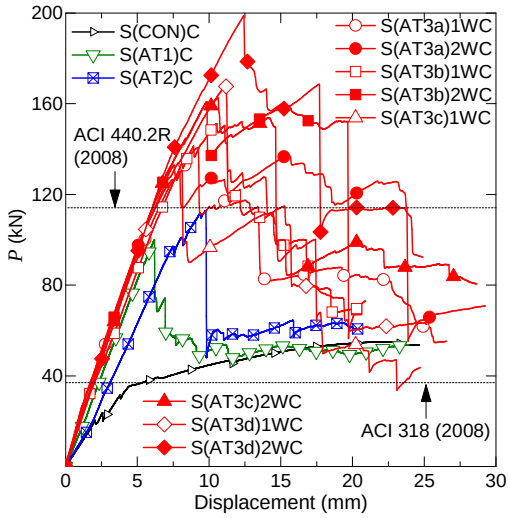

(c) Stone aggregate concrete (weak in compression)

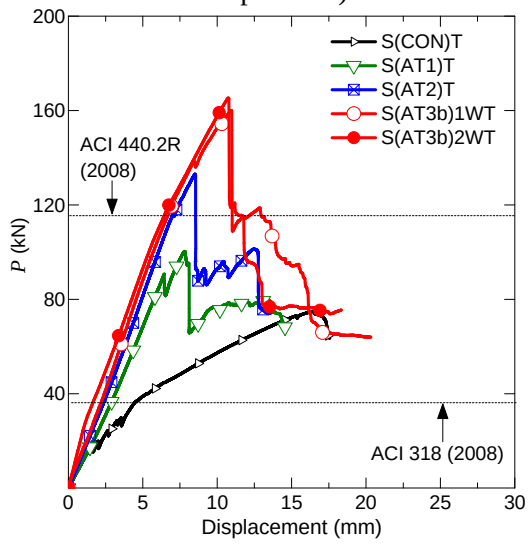

(d) Stone aggregate concrete (strong in compression)

Fig. 9. Load-displacement responses of beams fabricated using different anchorage schemes for brick and stone aggregate concrete beams. The notations are further defined in Figure 3.

This is the Post-print Version
Hasnat, A., Islam, M. M., & Amin, A. F. M. S. (2015). Enhancing the Debonding Strain Limit for CFRP-Strengthened RC Beams Using U-Clamps: Identification of Design Parameters. Journal of Composites for Construction. http://dx.doi.org/10.1061/(ASCE)CC.1943-5614.0000599

The beams in the AT3 group, with U-clamps, achieved the highest ultimate loads (Table 4) and the largest displacements at the peak load, P, whereas those in the AT1 group sustained the lowest, and the responses of the beams in the AT2 group fell in between. These observations demonstrate the role of an anchorage system in controlling the debonding phenomenon to achieve larger ultimate load capacities in strengthened beams. Furthermore, the unclamped strengthened beams (both AT1 and AT2) suffered from post-peak debonding failure characterized by instantaneous drops in the load-displacement responses caused by the separation of the concrete cover from the beam bottom. After such a drop, the load-displacement response was comparable to those recorded for the control (unstrengthened) beams, indicating the loss of the CFRP strengthening system. By contrast, the post-peak load-displacement responses in the U-clamped strengthened beams (AT3) were characterized by sequential failure with a progressive decrease in load, the behavior that is desired in any RC structure. However, after the loss of the external strengthening system, the load-displacement responses of the AT3 beams also followed a trend similar to that observed for the control beams.

The surface strains at the ultimate load, P, as measured across the depth are plotted in Figure 10 for beams having two different reinforcement schemes. The neutral axis was observed to move toward the top surface, resulting in a lower compression block area, in beams with less reinforcement in the compression zone. The tension block thus received a higher percentage of the strain compared with the compression block. This finding explains the crushing of the concrete in the compression zone when the concrete strain reaches its ultimate limit. The U-clamped specimens (AT3) sustained higher strain compared with the unclamped specimens (AT1). In several measurements, the strain across the depth was found not to be truly proportional over the depth in accordance with Navier's fundamental hypothesis. This may be attributable to the existence of material nonlinearity coupled with unavoidable errors in measuring the surface strain of a cracked system via video extensometry.

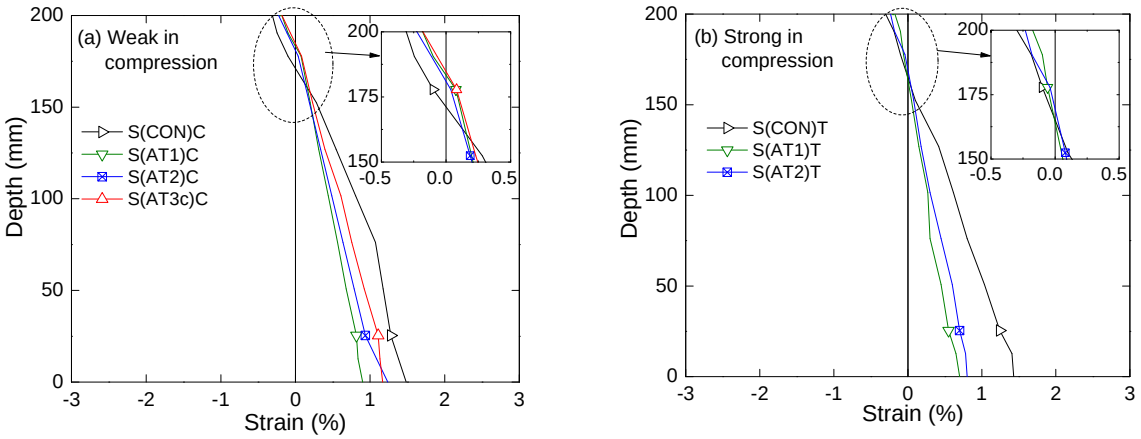

Fig. 10. Flexural strain and depth phenomena for different anchorage types: (a) weak compression zones (C) and (b) strong compression zones (T). The shift of the neutral axis is illustrated in the inset figures.

Effect of the coarse aggregate type and steel reinforcement strategy

Figure 11 presents the lines of parity drawn to illustrate the effect of the coarse aggregate type and reinforcement scheme on the experimentally recorded nominal moment capacity, M_n, calculated for the ultimate load, P. The parity plots show the gradual enhancement in moment

capacity achieved by changing the anchorage system from AT1 to AT3. However, closer inspection reveals that the stone aggregate concrete beams in the AT3 group sustained higher loads than did the brick aggregate concrete beams. The nominal moment capacity, M_n, was also found to be lower in the beams that were weaker in the compression zone. However, none of these differences is significant from the design perspective.

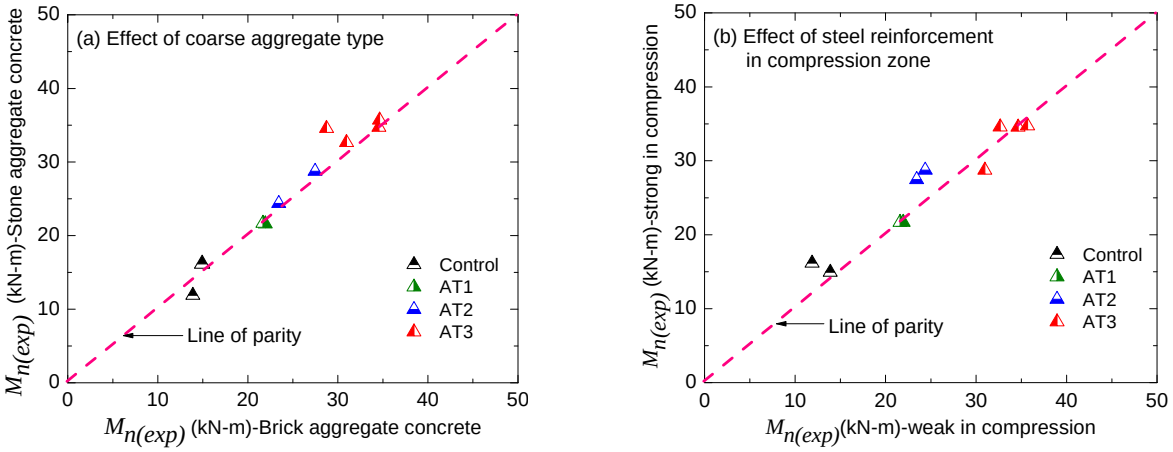

Fig. 11. Parameters affecting the moment capacities of CFRP-strengthened beams: (a) the effect of the coarse aggregate type and (b) the effect of steel reinforcement in the compression zone.

Effect of the anchorage type on flexural capacity

Figure 12 shows the effect of the anchorage type on the moment capacity enhancement for beams with weak compression zones (Figure 12a) and strong compression zones (Figure 12b). The trends of improvement indicated for the brick aggregate concrete beams (dotted lines) are lesser in magnitude than those observed for the stone aggregate concrete beams (solid lines) with the different U-clamp parameters in the AT3 scheme. The larger dilation (Islam et al. 2011, 2015) that occurs in brick aggregate concrete beams under the principal compression at the support (Figure 8) may play a role in causing the CFRP wraps to rupture at loads lower than those sustained by stone aggregate concrete beams. Furthermore, it is generally observed that in AT3c and AT3d, the nominal moment capacity, M_n, can be increased by increasing the U-clamp width along the beam axis, and the stiffness (a function of the wrap thickness, t_{fw}; the number of wrap layers, n_w; and the modulus of elasticity of the CFRP wrap, E_{fw}). However, the incorporation of an additional wrap at the mid-span (AT3b) or wrapping the full length of the beam (AT3a) offered no additional advantage compared with end wraps alone (AT3c and AT3d). These crucial observations clearly justify the initial supposition presented in Figures 1–2: U-clamps with unidirectional CFRP fibers aligned along the beam perimeter are effective only in the zone where the principal compression arch touches the beam bottom (tension face). Nevertheless, the physical evidence as explicitly observed in the experiments provides an avenue for the development of rational procedures for specifying U-clamp designs based on direct consideration of the stiffness parameters of CFRP wraps.

This is the Post-print Version
Hasnat, A., Islam, M. M., & Amin, A. F. M. S. (2015). Enhancing the Debonding Strain Limit for CFRP-Strengthened RC Beams Using U-Clamps: Identification of Design Parameters. Journal of Composites for Construction. http://dx.doi.org/10.1061/(ASCE)CC.1943-5614.0000599

EQUATIONS TO PREDICT DEBONDING STRAIN

The experimental results presented in the preceding section provide first-hand evidence of the role that U-clamps installed near the support play in increasing the moment capacity, M_n, of a CFRP plate-strengthened beam. Premature debonding failure is arrested through the introduction of partial confinement in stress localization zones where such failure is known to occur. Furthermore, the simple theoretical computational results presented in Figure 1 and analytical concept presented in Figure 2 for the principal stress distribution in compression arch zones of unclamped and clamped concrete beams conform closely to the experimental observations. In this context, this section is devoted to the proposal of relations to predict debonding strains in simply supported CFRP-strengthened beams U-clamped at the ends. The coefficients of the known relations for unclamped beams are also reevaluated.

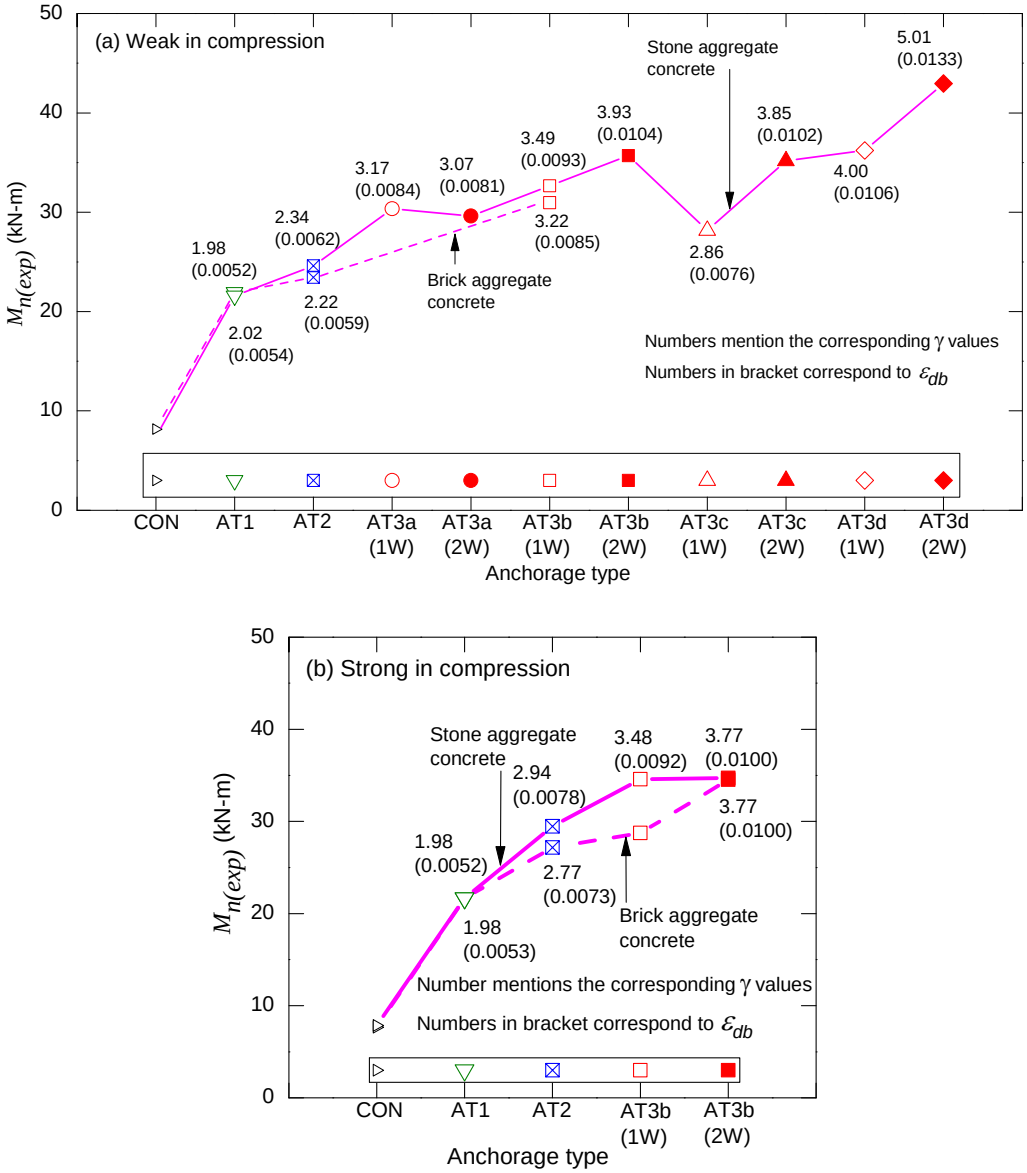

Fig. 12. Effect of the anchorage system on the moment capacity: (a) weak compression zones (C) and (b) strong compression zones (T).

To this end, the nominal moment capacity, M_n, of a CFRP-strengthened beam is expressed by Equation 1, where $M_{n(steel)}$ is the moment supported by the existing steel reinforcement and $M_{n(CFRP)}$ is the increase in moment capacity due to the incorporation of an externally bonded CFRP plate.

$$M_n = M_{n(steel)} + M_{n(CFRP)} \tag{1}$$

The determination of $M_{n(steel)}$ follows directly from ACI 318 (2008) using Equation 2.

$$M_{n(steel)} = A_s f_y \left(d_f - \frac{\beta_1 c}{2} \right) \tag{2}$$

where A_s is the area of steel reinforcement, f_y is the yield strength of the steel rebar, d_f is the effective depth of the flexural reinforcement, β_1 is the ratio of the depth of the equivalent rectangular stress block to the depth of the neutral axis and c is the distance from the extreme compression fiber to the neutral axis.

The contribution of $M_{n(CFRP)}$ to the flexural capacity enhancement is calculated using Equation 3 (ACI 440.2R 2008):

$$M_{n(CFRP)} = A_f f_{fe} \left(d_f - \frac{\beta_1 c}{2} \right) \tag{3a}$$

$$f_{fe} = E_f \varepsilon_{fe} \tag{3b}$$

$$\varepsilon_{fe} = 0.003 \left(\frac{d_f - c}{c} \right) \le \varepsilon_{db} \tag{3c}$$

where A_f is the area of the external CFRP reinforcement, f_{fe} is the effective stress in the CFRP, E_f is the tensile modulus of elasticity of the CFRP, ε_{fe} is the effective level of strain in the CFRP reinforcement attained at failure and ε_{db} is the debonding strain of the externally bonded CFRP reinforcement. Here, the authors take the original approach proposed in Toutanji et al. (2006), which is also partially followed in ACI 440.2R (2008) (see also Table 5). In this approach, the limiting debonding strain, ε_{db}, (Equation 3c) is generally specified as follows for two classes of concretes:

$$\varepsilon_{db} = \begin{cases} \gamma_L (t_f E_f)^{-0.5} & \text{for } f_c' \le 31.5\,\text{MPa} \\ \gamma_H (t_f E_f)^{-0.5} & \text{for } f_c' \ge 31.5\,\text{MPa} \end{cases} \tag{4a, 4b}$$

where γ_L and γ_H are the multiplicative factors for low-strength (L) and high-strength (H) concrete, respectively. In this study, considering the concrete strengths of the test beams, the

coefficients related to Equation 4b were estimated from the test dataset for the different anchorage types. The expressions corresponding to Equation 4b for AT1, AT2 and AT3 are as follows:

AT1: $$\varepsilon_{db} = \gamma_{H1}(n_f t_f E_f)^{-0.5},\ f_c^{'} \geq 31.5\,\text{MPa} \quad (5)$$

AT2: $$\varepsilon_{db} = \gamma_{H2}(n_f t_f E_f)^{-0.5},\ f_c^{'} \geq 31.5\,\text{MPa} \quad (6)$$

AT3: $$\varepsilon_{db} = (\gamma_{H1} + \gamma_{H3})(n_f t_f E_f)^{-0.5},\ f_c^{'} \geq 31.5\,\text{MPa} \quad (7)$$

where n_f is the number of CFRP plates attached to the tension face. The values of γ_{H1} and γ_{H2} can readily be obtained from Figure 12 using Equations 1–3 for the values of $(n_f t_f E_f)^{-0.5}$ used in the experiments reported in this paper. γ_{H1} and γ_{H2} were each calculated by taking the average value for 4 tested specimens (Table 4) - S(AT1)C, S(AT1)T, B(AT1)C and B(AT1)T for γ_{H1} and S(AT2)C, S(AT2)T, B(AT2)C and B(AT2)T for γ_{H2} - and the values were found to be 2.00 and 2.57, with coefficients of variation of 0.011 and 0.13, respectively. When compared with the debonding models presented in Table 5, the values are very close to those derived by Toutanji et al. (2006). The value prescribed by ACI 440.2R (2008) is larger than the current estimation, whereas the prescribed values of JSCE (2001), Maruyama and Ueda (2001) and Li et al. (2013) are considerably lower.

To identify the general dependence of the γ_{H3} parameter, the numerical procedure presented in Figure 1c was implemented for three arbitrarily varied confined compressive stresses and three CFRP U-clamp widths, w, where the latter is presented as a length ratio (the length of the U-clamp measured from the face of the support along the axis of the beam to the effective span of the beam).

Table 5. Debonding models for externally bonded CFRP strengthened beams without any end anchorage.

Model	Equation	Equivalent multiplier coefficient, γ for ε_{db} if $f_c^{'} = 48\,\text{MPa}$.
JSCE (2001)/ Maruyama and Ueda (2001)	$\varepsilon_{db} = \sqrt{2G_f / E_f t_f}$, $G_f = 0.50\,\text{N/mm}$	1.00
Toutanji et al. (2006)	$\varepsilon_{db} = \begin{cases} 0.08 f_c^{'}(t_f E_f)^{-0.5} & \text{for } f_c^{'} \leq 31.5\,\text{MPa} \\ 2.51(t_f E_f)^{-0.5} & \text{for } f_c^{'} \geq 31.5\,\text{MPa} \end{cases}$	2.51
ACI 440.2R (2008)	$\varepsilon_{db} = 0.41\sqrt{f_c^{'}/nE_f t_f} \leq 0.90\varepsilon_{fu}$	2.84
Li et al. (2013)	$F_d = \min(F_{e1}, F_{e2})$ $F_{e1} = b_f\sqrt{0.4E_f t_f f_t}$, $F_{e2} = f_t b_f L_e^2 / 6a_s$	1.02

G_f: interfacial fracture energy; t_f: nominal thickness of 1-ply of a CFRP plate; $f_c^{'}$: unconfined compressive strength of concrete determined per ASTM C39/C39M; n: number of CFRP plies; ε_{fu}: design rupture strain of the CFRP plate; f_t: tensile strength of concrete; b_f: width of the CFRP plate; L_e: effective bond length; E_f: tensile modulus of elasticity of CFRP; F_d: tensile force before the debonding of the CFRP sheet. Equations 4-7 are used for determining corresponding γ values reported in the table.

The segmental lengths of the two symmetrically stronger ends, w, of the simply supported beam were varied, and larger compressive strength values were arbitrarily assigned to these regions as parametric variations. The principal compressive stress values sampled at the support are plotted against the confined compressive strength (the compressive strength at the end parts) and w in Figures 13a and 13b. The results obtained from Figure 1b with no confinement are also plotted as the stress level at $w = 0$. These plots reveal a linear relation between the principal compressive stress and w (Figure 13a). A logarithmic relation of the form $y = A + Bx^{0.5}$ between the principal compressive stress and the confined compressive strength can be observed in Figure 13b. The stresses obtained from the numerical results that were used to plot 13a and 13b were taken at the same nodes representing the support locations in the mesh shown in Figure 1. The relations thus recovered from the analysis were derived from a concrete-only model, although the actual behavior of a CFRP-strengthened RC beam consisting of different materials with different moduli of elasticity, stiffnesses and interfacial properties is related to the interactions among the concrete, steel and CFRP. However, to remain consistent with the primary objective of this paper, the authors avoided the further complexities associated with truly understanding and modeling these complicated interfacial phenomena among the concrete, CFRP and steel in detail in their finite element model. Instead, the recovered relations were directly fitted to the experimental measurements to estimate the unknown coefficients (Figure 13c). This simplification neglects additional effects in the FE model, e.g., frictional slip, shear, adhesion, elastic mismatch, etc., that may be relevant in more accurate models; therefore, this approach may weaken the generalizability of the derived coefficients to other beam geometries, fiber orientations or reinforcement schemes. Nevertheless, the authors observe that the derived relations are analogous in form to those proposed by Toutanji et al. (2006) and partially followed in ACI 440.2R (2008).

Based on these revelations, the five experimental data points from the test specimens are plotted in Figure 13c; these data points consist of the average AT1 results [the average of four data points from the unclamped beams S(AT1)C, S(AT1)T, B(AT1)C and B(AT1)T] and the AT3 results [the data points are from S(AT3c)1WC, S(AT3c)2WC, S(AT3d)1WC, and S(AT3d)2WC]. A best fit of the linear relation between γ_{H3} and $w\sqrt{n_w t_{fw} E_{fw}}$ was obtained using the experimental data points, where n_w, t_{fw} and E_{fw} are the number of wraps, the thickness of the dry fabric and the modulus of elasticity of the dry fabric, respectively. The values of $w\sqrt{n_w t_{fw} E_{fw}}$ that were used in the plot were calculated from Table 3 and Figure 3. The obtained fit yielded the following relation:

$$\gamma_{H3} = \frac{w\sqrt{n_w t_{fw} E_{fw}}}{51} \tag{8}$$

where $w \leq$ the ratio of the length of the principal compressive force zone to the effective beam span.

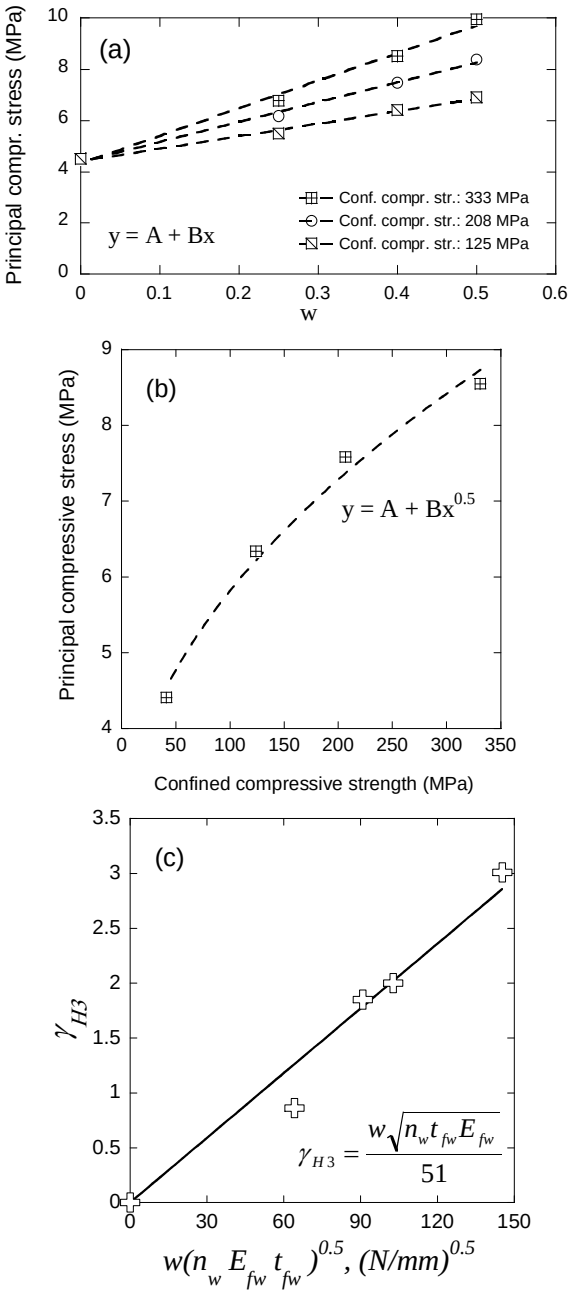

Fig. 13. Relations among the principal compressive stress, the normalized wrap length, the confined compressive strength, γ_{H3} and $w\sqrt{n_w t_{fw} E_{fw}}$: (a) principal compressive stress vs. normalized wrap length, (b) principal compressive stress vs. confined compressive strength, and (c) the proposed relation between γ_{H3} and $w\sqrt{n_w t_{fw} E_{fw}}$.

Equation 8 is specific to the particular orientation of the U-clamp fibers with respect to the direction of the principal compression stress that the fibers are resisting at the ends (installation location) in a simply supported RC beam. This equation also retains all relevant parameters of a confining pressure model for confined concrete. Consistent with the prevailing theories for

This is the Post-print Version
Hasnat, A., Islam, M. M., & Amin, A. F. M. S. (2015). Enhancing the Debonding Strain Limit for CFRP-Strengthened RC Beams Using U-Clamps: Identification of Design Parameters. Journal of Composites for Construction. http://dx.doi.org/10.1061/(ASCE)CC.1943-5614.0000599

predicting the confined compressive strengths of rectangular (noncircular) sections (ACI 440.2R 2008), the stress distribution arising for the case of partial confinement (Figure 2c), and consequently the presented coefficient in Equation 8, may be predominantly applicable to beams with the particular cross-sectional shape (Figure 4) tested in this investigation, with a width/depth (b/h) ratio of 0.75. Further verification for beams of different cross-sectional geometries may be important to experimentally confirm this hypothesis. This issue is further addressed in the last part of the next section.

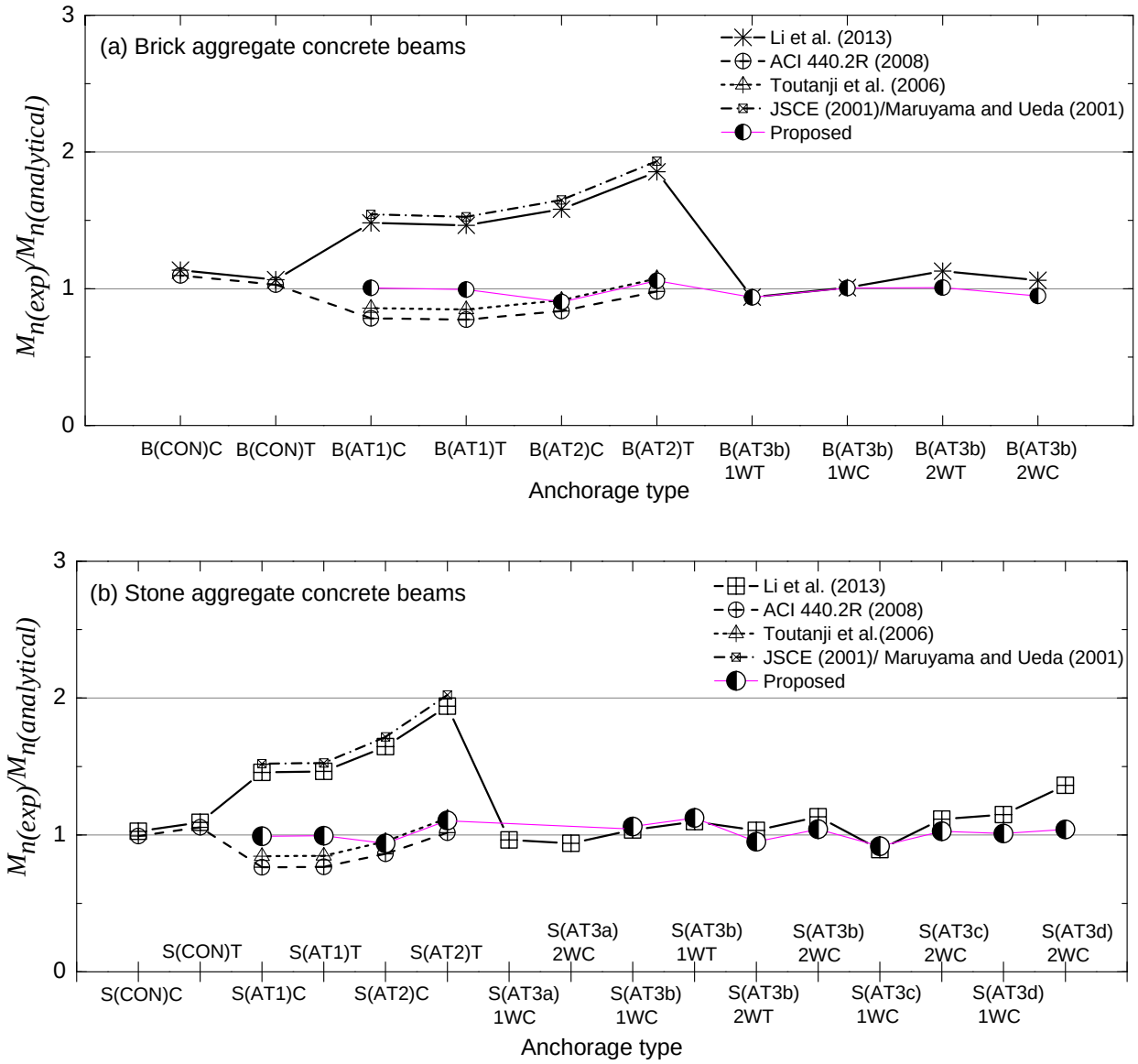

Fig. 14. Comparison of the moment capacities obtained from the experiments and through analytical calculations using available methods for the different anchorage types: (a) brick aggregate concrete beams and (b) stone aggregate concrete beams.

This is the Post-print Version
Hasnat, A., Islam, M. M., & Amin, A. F. M. S. (2015). Enhancing the Debonding Strain Limit for CFRP-Strengthened RC Beams Using U-Clamps: Identification of Design Parameters. Journal of Composites for Construction. http://dx.doi.org/10.1061/(ASCE)CC.1943-5614.0000599

TEST RESULTS COMPARED WITH THE LITERATURE

Figure 14 represents the ratios of the experimentally measured capacity to the analytically calculated capacities obtained using analytical models proposed by different researchers. Few analytical procedures are available in the literature for U-clamped cases. In this work, the procedures presented by Li et al. (2013) for low-strength concrete (considerably lower than 31.5 MPa) were also considered as methods for comparing the analytical capacities of the tested U-clamped and unclamped specimens. The suggested procedures of Li et al. (2013) and JSCE (2001), after Maruyama and Ueda (2001), underestimate the moment capacity and are conservative for all cases of unclamped beams. By contrast, the methods of Toutanji et al. (2006) and ACI 440.2R (2008) overestimate the actual capacity in all unclamped cases. The authors' model fits the experimental capacity well for the unclamped specimens. For the U-clamped cases, the analytical capacity evaluated using the method of Li et al. (2013) closely matched the actual capacity for a few cases (B(AT3b)1WC and S(AT3b)2WT), but it did not match for the cases in which the wrap width, w, and/or the wrap thickness, $n_w t_{fw}$, were varied in the specimens (S(AT3c)1WC, S(AT3c)2WC, S(AT3d)1WC and S(AT3d)2WC). By contrast, the authors' model was able to represent all cases except the specimens for which U-clamps were applied along the entire beam span (AT3a specimens) or mid-span (AT3b specimens).

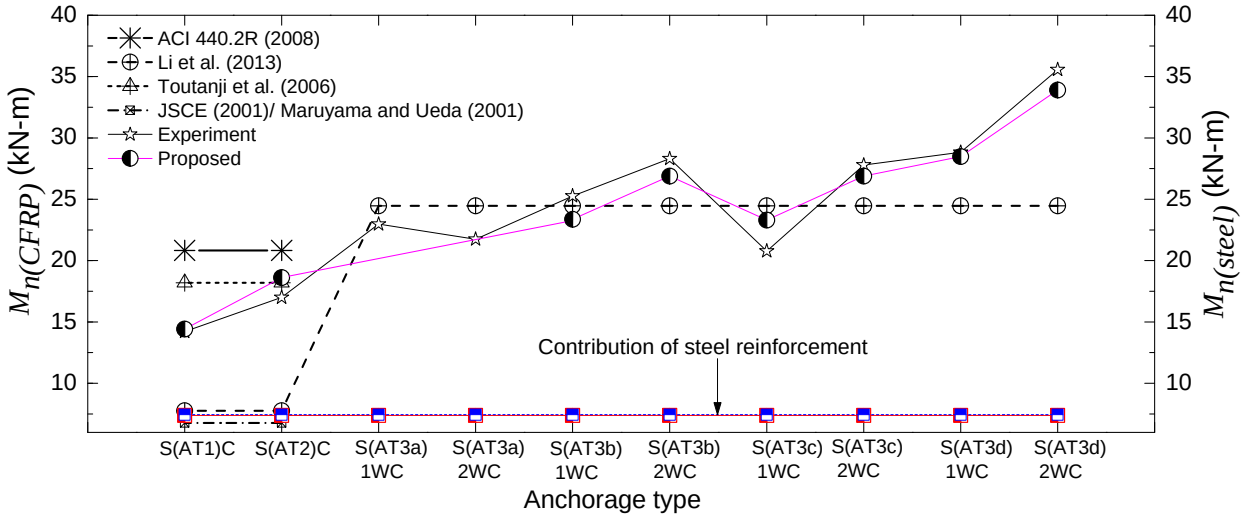

Fig. 15. Comparison of the contributions of the steel and the CFRP plates to the analytical moment capacities obtained using available methods for the different anchorage types for stone aggregate concrete beams.

However, the formulation presented by Li et al. (2013) does not contain any explicit terms to account for these factors when calculating M_n. Figure 15 further elucidates the situation by dividing the total moment capacity, $M_{n(\exp)}$, into $M_{n(steel)}$ and $M_{n(CFRP)}$. For plotting purposes, the theoretical moment capacity provided by the steel reinforcement, $M_{n(steel)}$, which was a constant value for all cases, was subtracted from the total experimental moment capacity, $M_{n(\exp)}$, to obtain $M_{n(CFRP)}$. The contributions of the CFRP plates were lower for the AT1 and AT2 schemes than for the AT3 scheme. However, the expressions provided by Li et al. (2013)

suggest the same value of $M_{n(CFRP)}$ in all cases, whereas the experimental values exhibit an increasing trend with increasing w and/or $n_w t_{fw}$ for the S(AT3c)1WC, S(AT3c)2WC, S(AT3d)1WC and S(AT3d)2WC cases. The model proposed by the authors (Equation 8) well captures these data points.

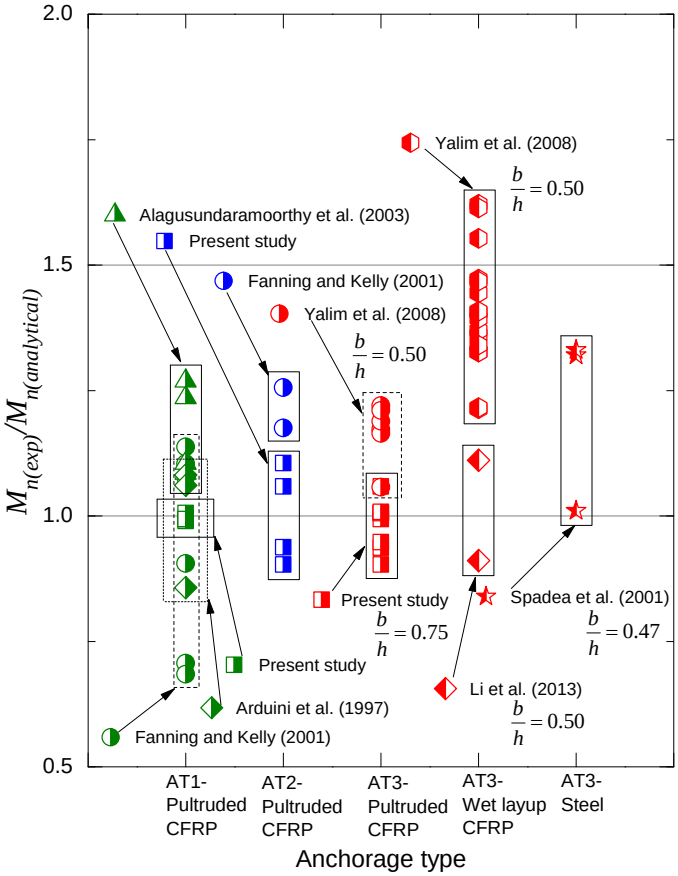

Fig. 16. Comparison of the authors' model with a database of published tests. The b/h ratios for the AT3 beams are also indicated (data from Alagusundaramoorthy et al. 2003; Fanning and Kelly 2001; Arduini et al. 1997; Yalim et al. 2008; Li et al. 2013; Spadea et al. 2001)

Finally, the test results published in different literatures were considered to evaluate the performance of the proposed model. In this evaluation, the differences among the test conditions established by the different research groups were considered for proper interpretation of the findings and to provide indications for further generalization of the proposed Equation 8 from an extended set of well-planned experiments. Figure 16 compares the published experimental results from 42 test beams. The differences observed between the predicted and experimental capacities can be attributed to the differences in the test schemes used. For AT1, the results of Arduini et al. (1997) and Fanning and Kelly (2001) correspond well to those obtained using the authors' model, with the exception of two data points from the latter. In these two cases, the CFRP plate lengths, which were shorter than the full lengths of the beams, resulted in lower $M_{n(\exp)}$ values. The authors' model appears to be conservative for the data from Alagusundaramoorthy et al. (2003), for which the wet lay-up technique was used. Only a few works can be found in the literature that corresponds to AT2. Fanning and Kelly (2001)

conducted experiments comparable to the AT2 specimens of this paper. The authors' model predicts these AT2 data in a conservative manner. Fanning and Kelly (2001) used 120 mm wide CFRP plates, whereas those in the current study were 100 mm in width, yielding a shorter end anchorage zone. Minor deviations are observed for the pultruded cases with U-clamped specimens tested by Yalim et al. (2008), in which three concrete surface conditions (smooth, slightly rough and rough) were used as test variables. Li et al. (2013) and Yalim et al. (2008) conducted AT3-like experiments using the wet lay-up technique. Their use of a lower b/h value (0.50) than that used by the authors (0.75) may have led to a larger confinement effect on the CFRP plates, which should have ultimately resulted in higher experimental moment capacities than those predicted by the proposed relation (Equation 8). However, only the test results of Yalim et al. (2008) support this proposition. Moreover, Spadea et al. (2001) used CFRP U-clamps to bond an externally mounted steel plate instead of a CFRP plate in the tension zone. Interestingly, the authors' model is consistent with only one test data point out of 3 identical test specimens. Furthermore, for the authors' results and the published results, the ratio of the CFRP plate width to the beam width ranged between 0.34 and 1.00. Even over this wide range of variation, although the appropriate CFRP plate width was used to derive the analytical moments, no logical trend of variation in $M_{n(\exp)}/M_{n(analytical)}$ is apparent in the context of the debonding phenomenon and its control.

CONCLUSIONS

1. The incorporation of CFRP wraps acting as U-clamps at the ends of a simply supported RC beam strengthened with CFRP plates can significantly increase the moment capacity by as much as 97% compared with unclamped beams by enhancing the debonding strain. Furthermore, progressive failures in U-clamped beams allowing for larger deflections (by up to 133% compared with unclamped beams) at ultimate load were observed, in contrast with the sudden failure exhibited by strengthened beams without any U-clamps.
2. The ultimate moment capacities of strengthened beams increase with increasing stiffness and width of the U-clamps installed near the support locations.
3. These significant observed performance enhancements are understood to be a result of the confinement effect of the CFRP wraps acting as U-clamps on the unconfined cover concrete at the two sides and bottom of the beam in combination with the externally bonded CFRP plates at the two ends of the beam in zones near the supports, where the compression arch meets the plate ends. Thus, CFRP wraps with fibers oriented around the beam perimeter provide a partial confinement effect at the bottom and sides of the beam ends by resisting the separation of the concrete cover. As a result, debonding failure occurs at a higher ultimate load.
4. In experiments on beams subjected to four-point loading, the incorporation of U-clamps at the mid-span, including wrapping spanning the full beam length, did not provide additional benefits in significantly increasing the moment capacity.
5. The clamping mechanism that contributes to delaying debonding failure was interpreted based on the observed failure patterns, the principal compressive stress distributions of the loaded beams and the partial confinement effect that prevailed in the compression zone as a result of the U-clamps. Based on these assessments, the required locations and extents of CFRP wraps serving as U-clamps can be determined. The effect of the b/h ratio on inducing

effective confinement was evaluated based on the test data presented in the paper together with previously published test results.

6. A relation was proposed to predict the moment capacities of simply supported RC beams strengthened with externally bonded pultruded CFRP plates based on the width and stiffness properties of the CFRP-wrap U-clamps installed at the ends. The coefficients of the existing relations proposed by Toutanji et al. (2006) for unclamped beams were also reevaluated based on the authors' test data.
7. The test data suggest the existence of a pseudo-dilation effect in brick aggregate concrete beams caused by U-clamp confinement in the compression zone. However, the constructed parity plots show insignificant effects of coarse aggregate or steel reinforcement on the ultimate moment capacities of the strengthened test beams from the design point of view.
8. The test results, equations and estimated coefficients presented in this paper are specific to the materials, geometry, support condition, loading conditions, fiber orientations, plate widths and sectional properties of the test beams. Nevertheless, the fundamental fact of the necessity of effectively confining the compression arch in any shallow beam inspires the authors to believe that the generally applicable concepts and procedures presented here bear a broader significance for future experimental and numerical studies of continuous span beams and other different support conditions and loading conditions as well as beams with other b/h ratios. The methodology of using bidirectional fibers, particularly to confine the mid-span zone, is worth exploring in the future.

Acknowledgments

The authors are grateful to the members and staff of the Concrete Laboratory and Structural Mechanics Laboratory, Department of Civil Engineering, Bangladesh University of Engineering and Technology for their support and cooperation in conducting the tests. The authors gratefully acknowledge the kind cooperation extended by LaMaCo System Sdn Bhd, Malaysia, who provided samples of the fiber-reinforced polymer wraps used in this investigation. Special thanks go to Ratanpur Steel Re-Rolling Mills Ltd. and Shun Shing Group, who provided the steel reinforcements and cement, respectively. The authors also sincerely appreciate the funding provided by the Committee for Advanced Studies and Research, BUET, Dhaka, Bangladesh, and the technical support of the Bangladesh Bridge Authority and M/S Aziz & Company Limited, Dhaka, Bangladesh, for this research.

REFERENCES

ACI 318 (2008). "Building code requirements for structural concrete." American Concrete Institute, Farmington Hills, MI, 2008.

ACI 440.2R (2008). "Guide for the design and construction of externally bonded FRP systems for strengthening concrete structures." American Concrete Institute, Farmington Hills, MI, 2008.

Akhtaruzzaman, A. A., and Hasnat, A. (1983). "Properties of concrete using crushed brick as aggregate." Concrete International, 5(2), 58-63.

Akhtaruzzaman, A. A., and Hasnat, A. (1986). "Shear and flexural behavior of brick-aggregate concrete beams without web reinforcement." ACI Journal Proceedings, 83(2). 284-289.

Algusundaramoorthy, P, Harik, IE, and Choo, CC. (2003). "Flexural behavior of R/C beams strengthened with CFRP sheets or fabric." Journal of Composites for Construction, 7(4), 292-301.

Al-Tamimi, A. K., Hawileh, R., Abdalla, J., and Rasheed, H. A. (2011). "Effects of ratio of CFRP plate length to shear span and end anchorage on flexural behavior of SCC RC beams." Journal of Composites for Construction, 15(6), 908-919.

ANSYS 11 [Computer software]. Houston, PA, Swanson Analysis Systems.

Arduini, M., Di Tommaso, A., and Nanni, A. (1997). "Brittle failure in FRP plate and sheet bonded beams." ACI Structural Journal, 94(4), 363-370.

ASTM C150 / C150M (2012). "Standard Specification for Portland Cement." American Society for Testing and Materials, 100 Barr Harbor Drive, PO Box C700, West Conshohocken, PA, 19428-2959 USA.

ASTM C39 / C39M (2014). "Standard test method for compressive strength of cylindrical concrete specimens." American Society for Testing and Materials, 2003. American Society for Testing and Materials, 100 Barr Harbor Drive, PO Box C700, West Conshohocken, PA, 19428-2959 USA.

ASTM C496 / C496M (2011). "Standard test method for splitting tensile strength of cylindrical concrete specimens." American Society for Testing and Materials, 100 Barr Harbor Drive, PO Box C700, West Conshohocken, PA, 19428-2959 USA.

ASTM D3039 / D3039M (2014). "Standard test method for tensile properties of polymer matrix composite materials." American Society for Testing and Materials, 2003. American Society for Testing and Materials, 100 Barr Harbor Drive, PO Box C700, West Conshohocken, PA, 19428-2959 USA.

ASTM D638 (2010). "Standard test method for tensile properties of plastic." American Society for Testing and Materials, 2003. American Society for Testing and Materials, 100 Barr Harbor Drive, PO Box C700, West Conshohocken, PA, 19428-2959 USA.

ASTM D4541 (2009). "Standard test method for pull-off strength of coatings using portable adhesion testers." American Society for Testing and Materials, 2003. American Society for Testing and Materials, 100 Barr Harbor Drive, PO Box C700, West Conshohocken, PA, 19428-2959 USA.

Bencardino, F., Spadea, G., and Swamy, R. N. (2002). "Strength and ductility of reinforced concrete beams externally reinforced with carbon fiber fabric." ACI Structural Journal, 99(2), 163-171.

Bower, J. E., and Viest, I. M. (1960). "Shear strength of restrained concrete beams without web reinforcement." ACI Journal Proceedings, 57(7), 73-98.

Braga, F. Gigliotti, R. and Laterza, M. (2006). "Analytical stress strain relationship for concrete confined by steel stirrups and/or FRP jackets." Journal of Structural Engineering, 132(9), 1402-1416.

Buyukozturk, O., Gunes, O., and Karaca, E. (2004). "Progress on understanding debonding problems in reinforced concrete and steel members strengthened using FRP composites." Construction and Building Materials, 18(1), 9-19.

Chajes, M. J., Thomson Jr, T. A., Januszka, T. F., and Finch Jr, W. W. (1994). "Flexural strengthening of concrete beams using externally bonded composite materials." Construction and Building Materials, 8(3), 191-201.

Choudhury, M. S. I. (2012). "Confinement effect of fiber reinforced polymer wraps on circular and square concrete columns." M.Sc. thesis, Dept. of Civil Engineering, Bangladesh Univ. of Engineering and Technology, Dhaka, Bangladesh.

Debieb, F. and Kenai, S. (2008). "The use of coarse and fine crushed bricks as aggregate in concrete." Construction and Building Materials, 22(5), 886-893.

Dong, J., Wang, Q., and Guan, Z. (2013). "Structural behaviour of RC beams with external flexural and flexural–shear strengthening by FRP sheets", Composites Part B: Engineering, 44(1), 604-612.

El-Mihilmy, M. T., and Tedesco, J. W. (2001). "Prediction of anchorage failure for reinforced concrete beams strengthened with fiber-reinforced polymer plates." ACI Structural Journal, 98(3), 301-314.

Esfahani, M. R., Kianoush, M. R., and Tajari, A. R. (2007). "Flexural behaviour of reinforced concrete beams strengthened by CFRP sheets", Engineering Structures, 29(10), 2428-2444.

Fanning, P. J., and Kelly, O. (2001). "Ultimate response of RC beams strengthened with CFRP plates." Journal of Composites for Construction, 5(2), 122-127.

fib (2001). "Externally bonded FRP reinforcement for RC structures." Bulletin 14, Technical Report on the Design and Use of Externally Bonded Fiber Reinforced Polymer Reinforcement for Reinforced Concrete Structures, International Federation for Structural Concrete, Lausanne, Switzerland.

Girgin, Z. C. (2009). "Modified failure criterion to predict ultimate strength of circular columns confined by different materials." ACI Structural Journal, 106(6), 800-809.

Hasnat, A. (2014). "Experimental investigation on flexural capacity of reinforced concrete beams strengthened with carbon fiber reinforced polymer strips." M.Sc. Engg. Thesis, Department of Civil Engineering, Bangladesh University of Engineering and Technology, Dhaka, Bangladesh.

Hussain, M., Sharif, A., Baluch, I. B. M., and Al-Sulaimani, G. J. (1995). "Flexural behavior of precracked reinforced concrete beams strengthened externally by steel plates." ACI Structural Journal, 92(1), 14-23.

Islam, M.M., Choudhury, M.S.I., Abdulla, M., and Amin, A.F.M.S. (2011). "Confinement effect of fiber reinforced polymer wraps in circular and square concrete columns." 4th Annual Paper Meet and 1st Civil Engineering Congress, The Institution of Engineers (IEB), Dhaka, Bangladesh, 359–362.

Islam, M.M., Choudhury, M.S.I., and Amin, A.F.M.S. (2015). "Dilation effects in FRP-confined Square Concrete Columns using Stone-, Brick- and Recycled Coarse Aggregates." Journal of Composites for Construction, 10.1061/(ASCE)CC.1943-5614.0000574, 04015017.

Japan Society of Civil Engineers (JSCE) (2001). "Recommendations for the upgrading of concrete structures with use of continuous fiber sheets." Concrete Engineering Series 41, Tokyo.

Kalfat, R., Al-Mahaidi, R., and Smith, S. T. (2011). "Anchorage devices used to improve the performance of reinforced concrete beams retrofitted with FRP composites: State-of-the-art review." Journal of Composites for Construction, 17(1), 14-33.

Kani, G. N. J. (1964). "The riddle of shear failure and its solution." ACI Journal Proceedings, 61(4), 441-467.

Khalaf, F.M. (2006). "Using Crushed Clay Brick as Coarse Aggregate in Concrete." Journal of Materials in Civil Engineering, 18(4), 518-526.

Khalaf, F.M. and DeVenny, A.S.(2005). "Properties of new and recycled clay brick aggregates for use in concrete." Journal of Materials in Civil Engineering, 17(4), 456-464.

Li, X., Gu, X., Song, X., Ouyang, Y., and Feng, Z. (2013). "Contribution of U-shaped strips to the flexural capacity of low-strength reinforced concrete beams strengthened with carbon fibre composite sheets." Composites Part B: Engineering, 45(1), 117-126.

Lu, X. Z., Teng, J. G., Ye, L. P., and Jiang, J. J. (2005). "Bond–slip models for FRP sheets/plates bonded to concrete." Engineering Structures, 27(6), 920-937.

Malek, A. M., Saadatmanesh, H., and Ehsani, M. R. (1998). "Prediction of failure load of R/C beams strengthened with FRP plate due to stress concentration at the plate end." ACI structural Journal, 95(2), 142-152.

Mansur, M.A., Wee, T.H., and Cheran, L.S. (1999). "Crushed bricks as coarse aggregate for concrete." ACI Materials Journal, 96(4), 478-484.

Maruyama, K., and Ueda, T. (2001). "JSCE design recommendations for upgrading of RC member by FRP sheet." Proc., 5th Int. Symp. On Fiber Reinforced Concrete Structures, Cambridge, 441–446.

Mirmiran, A. and Shahawy, M. (1997a). "Dilation characteristics of confined concrete."Mechanics of Cohesive-Frictional Materials, 2(3), 237–249.

Mirmiran, A. and Shahawy, M. (1997b)."Behavior of concrete columns confined by fiber composites." Journal of Structural Engineering, 123(5), 583–590.

Mirmiran, A., Shahawy, M., Samaan, M., Echary, H. E., Mastrapa, J. C., and Pico, O. (1998). "Effect of column parameters on FRP-confined concrete." Journal of Composites for Construction, 2(4), 175-185.

Moran, D. A. and Pantelides, P. C. (2005). "Damage-based stress-strain model for fiber-reinforced polymer-confined concrete." ACI Structural Journal, 102(1), 54-61.

Pessiki, S., Harries, K. A., Kestner, J. T., Sause, R. and Ricles, J. M. (2001). "Axial behavior of reinforced concrete columns confined with FRP jackets." Journal of Composites for Construction, 5(4), 237-245.

Roberts, T. M. and Hajikazemi, H. (1989). "Theoretical Study of The Behaviour of Reinforced Concrete Beams Strengthened by Externally Bonded Steel Plates", ICE Proceedings, Thomas Telford, 87(1), 39-55.

Saadatmanesh, H. and Malek, A. M. (1998). "Design guidelines for flexural strengthening of RC beams with FRP plates." Journal of Composites for Construction, 2(4), 158-164.

Smith, S. T. and Teng, J. G. (2002a). "FRP-strengthened RC beams. I: review of debonding strength models." Engineering Structures, 24(4), 385-395.

Smith, S. T., and Teng, J. G. (2002b). "FRP-strengthened RC beams. II: assessment of debonding strength models." Engineering Structures, 24(4), 397-417.

So, M., and Harmon, T. G. (2008). "Cover delamination of reinforced concrete members with surface-mounted fiber-reinforced polymer reinforcement." ACI Structural Journal, 105(2), 196-204.

Soroushian, P., Choi, K. B., Park, G. H., and Aslani, F. (1991). "Bond of deformed bars to concrete: effects of confinement and strength of concrete." ACI Materials Journal, 88(3), 227-232.

Spadea, G., Swamy, R. N., and Bencardino, F. (2001). "Strength and ductility of RC beams repaired with bonded CFRP laminates." Journal of Bridge Engineering, 6(5), 349-355.

Swamy, R. N., Mukhopadhyaya, P., and Lynsdale, C. J. (1999). "Strengthening for shear of RC beams by external plate bonding." Structural Engineer, 77(12), 19-30.

Teng, J. G. and Yao, J. (2007). "Plate end debonding in FRP-plated RC beams—II: Strength model", Engineering Structures, 29(10), 2472-2486.

Teng, J. G., Smith, S. T., Yao, J., and Chen, J. F. (2003). "Intermediate crack-induced debonding in RC beams and slabs." Construction and building materials, 17(6), 447-462.

Toutanji, H., Zhao, L., and Anselm, E. (2006). "Verifications of design equations of beams externally strengthened with FRP composites", Journal of Composites for Construction, 10(3), 254-264.

Toutanji, H., Han, M. Gilbert, J. and Matthys, S. (2010). "Behavior of large scale rectangular columns confined with FRP composites." Journal of Composites for Construction, 14(1), 62-71.

Triantafillou, T. C. (1998). "Shear Strengthening of Reinforced Concrete Beams using Epoxy-Bonded FRP Composites." ACI Structural Journal, 95(2), 107-115.

Wu, Y. F., and Wei, Y. Y. (2010). "Effect of cross-sectional aspect ratio on the strength of CFRP-confined rectangular concrete columns." Engineering Structures, 32(1), 32-45.

Yalim, B., Kalayci, A. S., and Mirmiran, A. (2008). "Performance of FRP-strengthened RC beams with different concrete surface profiles." Journal of Composites for Construction, 12(6), 626-634.

Yao, J. and Teng, J. G. (2007). "Plate end debonding in FRP-plated RC beams—I: Experiments." Engineering Structures, 29(10), 2457-2471.